Hydrol. Earth Syst. Sci., 29, 5975–6001, 2025 https://doi.org/10.5194/hess-29-5975-2025 © Author(s) 2025. This work is distributed under the Creative Commons Attribution 4.0 License.





The hydrological archetypes of wetlands

Abigail E. Robinson¹, Anna Scaini¹, Francisco J. Peña², Peter A. Hambäck³, Christoph Humborg⁴, and Fernando Jaramillo¹

¹Department of Physical Geography, Stockholm University, Stockholm, 106 91, Sweden

Correspondence: Abigail E. Robinson (abigail.robinson@natgeo.su.se)

Received: 17 October 2024 - Discussion started: 2 December 2024

Revised: 18 August 2025 - Accepted: 31 August 2025 - Published: 4 November 2025

Abstract. Wetlands are valuable and diverse environments that contribute to a vast range of ecosystem services, such as flood control, drought resilience, and carbon sequestration. The provision of these ecosystem services depends on their hydrological functioning, which refers to how water is stored and moved within a wetland environment. Since the hydrological functions of wetlands vary widely based on location, wetland type, hydrological connectivity, vegetation, and seasonality, there is no single approach to defining these functions. Consequently, accurately identifying their hydrological functions to quantify ecosystem services remains challenging. To address this issue, we investigate the hydrological regimes of wetlands, focusing on water extent, to better understand their hydrological functions. We achieve this goal using Sentinel-1 SAR imagery and a self-supervised deep learning model (DeepAqua) to predict surface water extent for 43 Ramsar sites in Sweden between 2020 and 2023. Clustering analysis grouped the wetlands based on the water extent predictions into five archetypes based on their hydrological similarity: "spring-surging", "spring-flooded", "summerflooded", "slow-drying", and "summer-dry". The archetypes represent great heterogeneity, with flashy regimes being more prominent at higher latitudes and smoother regimes found preferentially in central and southern Sweden. Additionally, many wetlands show exceptional similarity in the timing and duration of flooding and drying events, which only became apparent when grouped. We attempt to link hydrological functions to the archetypes, whereby headwater wetlands, such as spring-surging wetlands, have the potential to accentuate floods and droughts, while slow-drying wetlands, typical of floodplain wetlands, are more likely to

provide services such as flood attenuation and water storage during low flow conditions. Additionally, although wetlands can be classified in a myriad of ways, we propose that classifying wetlands based on the hydrological regime derived from water surface extent is useful for identifying hydrological functions specific to the site and season and when discharge or water level data are not available. Lastly, we foresee that hydrological-regime-based classification can be easily applied to other wetland-rich landscapes to better understand the hydrological functions and identify their respective ecosystem services.

1 Introduction

Wetlands are ecosystems that are seasonally or permanently covered by or saturated with water (Bullock and Acreman, 2003). After centuries of wetland loss (Fluet-Chouinard et al., 2023), wetlands are now viewed as key providers of provisioning and regulating services such as forestry, fishing, food production, flood control, drought resilience, nutrient and sediment retention, and carbon sequestration (Ameli and Creed, 2019; Barbier et al., 1997; Colvin et al., 2019; Johnston, 1991; Matthew et al., 2010; Tang et al., 2020; Villa and Mitsch, 2015). Additionally, they offer cultural and supporting services (Margaryan et al., 2022; Mitsch et al., 1991; Wood et al., 2024) and are crucial for achieving the sustainable development goals outlined in Agenda 2030 (Jaramillo et al., 2019).

²Division of Health Informatics and Logistics, KTH Royal Institute of Technology, Stockholm, 171 77, Sweden

³Department of Ecology, Environment and Plant Sciences, Stockholm University, Stockholm, 106 91, Sweden

⁴Baltic Sea Centre, Stockholm University, Stockholm, 106 91, Sweden

The degree to which wetland environments provide ecosystem services is largely controlled by their hydrological functions (Okruszko et al., 2011) or how wetlands store and transfer water. For instance, hydrological functions such as prolonged water storage contribute to services like flood control and sustaining water supply during low flow periods (Åhlén et al., 2020; Bullock and Acreman, 2003; Gerakes, 1992). Other functions, such as surface-groundwater exchange, relate to provisioning services such as water supply, while surface wetness and soil moisture help regulate the local climate and retain nutrients (Ameli and Creed, 2017; Hansson et al., 2005; Le and Kumar, 2014; Mitsch et al., 2015). Furthermore, large fluctuations of surface water extent are strongly correlated to fluctuations of methane emissions for boreal wetlands (north of 50° N), which is important for services like carbon sequestration (Ringeval et al., 2010).

Quantifying the hydrological functions of wetlands and the provision of ecosystem services is challenging, as wetlands are spatiotemporally variable and diverse (McLaughlin and Cohen, 2013). For example, a wetland can either reduce or enhance flooding downstream depending on the environmental setting or time of year (Bullock and Acreman, 2003). One way to improve our understanding of wetland hydrological functions and related ecosystem services is by quantifying their hydrological regime. This refers to the seasonal availability of water (level, extent, or volume) within a wetland, measured through either in situ or remote sensing technologies (Acreman and Holden, 2013; Helmschrot, 2016).

The analysis of hydrological regimes to understand hydrological functioning usually focuses on rivers and catchments (Magilligan and Nislow, 2005; Robinson and Sivapalan, 1997). However, over the last two decades, its application for wetlands has steadily increased (e.g. Cuevas et al., 2024; Stevaux et al., 2020; Na and Li, 2022; Vilardy et al., 2011). In fact, methods for studying water extent have been driven by the need to quantify ecosystem services (Park et al., 2022). For instance, by monitoring water level or extent, we can evaluate whether a wetland is in a water-storing or water-transmitting state, which influences its ability to attenuate high flows downstream (Spence et al., 2011; Yanfeng and Guangxin, 2021). Furthermore, analysis of the hydrological regimes based on water extent and level in Siberian wetlands has enhanced the understanding of how water availability in winter influences spring flooding (Zakharova et al., 2014). In Europe, Vera-Herrera et al. (2021) demonstrated that grouping wetlands based on their long-term changes in surface water extent can help to maximize agricultural productivity, while Åhlén et al. (2022) distinguished between the flood buffering capacity of wetlands in upland and downstream wetlands by studying variations in water level.

When in situ water level or discharge measurements from water gauges are spatiotemporally sparse, water surface extent can be used to understand the hydrological regime. Estimating hydrological regimes from water surface extent is achievable with remote sensing technologies, such as optical or synthetic aperture radar (SAR) (Graversgaard et al., 2021; Ramsar Convention, 2011; Vera-Herrera et al., 2021). For example, multi-spectral optical sensors like Sentinel-2 can help estimate surface water extent at a resolution of 10 m (Brown et al., 2022). Others have exploited the ability of SAR to detect water below flooded vegetation in a range of wetland environments at similar resolutions (Canisius et al., 2019; Kovacs et al., 2013; Melack and Hess, 2011; Widhalm et al., 2015; Peña et al., 2024).

It is widely recognized that although ecosystem services are not undervalued, they are often poorly characterized and understood in the context of wetlands. Furthermore, generalizing hydrological functions and services across different wetlands is not recommended due to their unique characteristics. Here, we quantify changes in water surface extent to understand the hydrological regimes of wetlands and determine their hydrological functions using the case of Sweden. This study aims to categorize wetlands by their hydrological regime based on recent water surface extent observations using remote sensing data and a pre-trained selfsupervised deep learning model called DeepAqua (Peña et al., 2024). We use the case of 43 Ramsar wetlands as they are well-inventoried, present good spatiotemporal coverage of SAR data, and are of national and international importance due to the ecosystem services they provide (Gunnarsson and Löfroth, 2014; Ramsar Convention, 2011). We propose that by grouping hydrologically similar sites into descriptive archetypes (as suggested by Lane et al., 2018), more comprehensive insights can be gained about the hydrological regime (and thus functions) than by studying each wetland's hydrological regime in isolation.

2 Methods

2.1 Wetland dataset description

Sweden has 68 Ramsar wetlands in total (Ramsar Convention, 1971). For this study, we first excluded coastal sites because coastal wetlands are hydrologically different from inland wetlands and should therefore be studied separately. Sites with a total area exceeding 180 000 ha were also excluded due to computational and memory limitations when predicting water extent with deep learning. Further exclusions were made for sites with low SAR data availability, defined here as fewer than one acquisition every 14 d, resulting from processing challenges such as significant orbit gaps, incomplete bursts, and the loss of Sentinel-1B in December 2021. This left 43 Ramsar sites suitable for hydrological regime analysis, and each site was delimited based on the boundaries of the Ramsar Convention (Ramsar Convention Secretariat, 2023) (Fig. 1).

The sites are distributed throughout all regions in Sweden, albeit with a higher concentration of sites in central and southern Sweden. Site areas range between 200 and

28 900 ha and encompass various wetland types, including marshes, fens, bogs, mires, palsa mires, lakes, streams, wetland forests, peatlands, and shrub wetlands. For these wetlands, during the observation period (2020–2023), the average temperature and precipitation were 5.76 °C and 706.5 mm, which were 0.68 °C warmer and 25.6 mm wetter on average compared to the 1990–2020 climate normal (Johansson, 2002). Additionally, the mean number of snow days in Sweden between 2020 and 2023 was 108.0, which is 12.3 d less compared to the last climate normal (Swedish Meteorological and Hydrological Institute, 2024). Daily precipitation from the Copernicus Climate Change Service E-OBS ensemble (0.1° grid) for each Ramsar site is available in Figs. A7–A11 (Cornes et al., 2018).

2.2 Wetland characteristics

To place the wetlands into an environmental context, we tabulated each site's latitude, elevation, open water as a percentage of the total area, and general wetland type (Fig. 8). The elevation was calculated as the average elevation (m.a.s.l) derived from the Digital Elevation Model 50 m (Markhöjdmodell Nedladdning, grid 50+) (Lantmateriet, 2022) within the wetland boundary. Open water extent for each wetland was calculated as an average over all months in 2023 using monthly composites of normalized difference water index (NDWI) binary (water/non-water) masks from Sentinel-2 optical imagery.

The wetland type was estimated using the following databases of wetland classification: (1) the Ramsar Convention database for sites in Sweden, (2) the National Wetland Inventory for Sweden (VMI) (Gunnarsson and Löfroth, 2009), and (3) an updated satellite-based open wetland mapping classification from 2018-2022 (Hahn and Wester, 2023). Each wetland was assigned a generic wetland class adapted from Gunnarsson and Löfroth (2014): "open", "limnic", "mixed", or "mire". "Open" refers to meadows, grasslands, and temporarily flooded land, while "limnic" refers to lake shores, beaches by watercourses, overgrown lakes, and limnogeneous beach complexes. "Mixed" wetlands are regarded as a combination of multiple wetland types and may include different mires with open or limnic wetland environments. A "mire" wetland consists primarily of bogs and fens. A fifth wetland type, "fjäll" (mountain), was assigned to wetlands located in Sweden's mountainous regions as they are not classified in the datasets.

2.3 Hydrological regime given by water surface extent analysis

We estimated the hydrological regime from water extent using an automated approach based on remote sensing data. Automatic surface water detection was done with a deep learning image segmentation model called DeepAqua (Peña et al., 2024). DeepAqua is a self-supervised model whose

principal function is to detect surface water extent in wetlands from Sentinel-1 SAR imagery in the VH polarization. DeepAqua can detect both open and vegetated water using the C-band SAR sensor on board Sentinel-1, which can penetrate some types of perennial vegetation due to its emission of longer-wavelength radar waves (5.6 cm) (Adeli et al., 2021). Usually, semantic segmentation models require manually labelled images as their training label output. With DeepAqua, however, the training labels are binary images (water/nonwater) of the NDWI based on cloud-free Sentinel-2 optical imagery of the same location and time as the input training data (SAR imagery), since both missions have a ~ 1 week repeat cycle over Sweden (~1-2 passes per week between 2020 and 2022, after which spatiotemporal coverage is reduced to ~ 10 –12 d due to the failure of the Sentinel-1B satellite). For our analysis, we applied the pre-trained DeepAqua model (version name: "big-2020") without any fine-tuning. The model was originally trained on a Sentinel-1- and Sentinel-2-based NDWI binary image over central Sweden from the 5 June 2018. When the pre-trained model was tested on three wetlands in Sweden (Peña et al., 2024), DeepAqua outperformed existing land classification models such as Dynamic World (Brown et al., 2022) and thresholding techniques such as Otsu (Otsu, 1979) on multiple evaluation metrics such as pixel accuracy, intersection over union, precision, and F_1 .

The SAR imagery used as input to DeepAqua for surface water detection was obtained from Google Earth Engine following basic pre-processing steps: orbit file correction, border noise removal, thermal noise removal, and orthorectification. The output predictions comprised polygonized binary water/non-water images for every Sentinel-1 image available between January 2020 and August 2023, cropped to within the boundaries of each wetland. The total water area for each image was calculated based on the WGS84 UTM Zone 33N projection (Figs. A2–A6). The monthly average water extent between January 2020 and August 2023 was calculated to reduce the risk of annual variability affecting potential clustering while aiming to detect hydrological regimes under "average" conditions. Due to extensive snow and ice cover complicating the water extent predictions, winter months (November, December, January, and February) were removed from the hydrological regime analysis. All water extent data and corresponding SAR acquisition dates are provided in the Supplement.

Lastly, due to the lack of ground-truth data on temporally dynamic wetland water extent within our Ramsar sites, we validate our water extent predictions using two alternative approaches. Firstly, we compare DeepAqua's predicted water extent with manually delineated water extent derived from Sentinel-1 SAR imagery in the VH polarization for a systematic sample of wetlands for all available images during 2021. To ensure a representative yet unbiased sample, we selected one wetland from each resulting archetype, covering a broad range of wetland types, sizes, and latitudes. Manual delin-

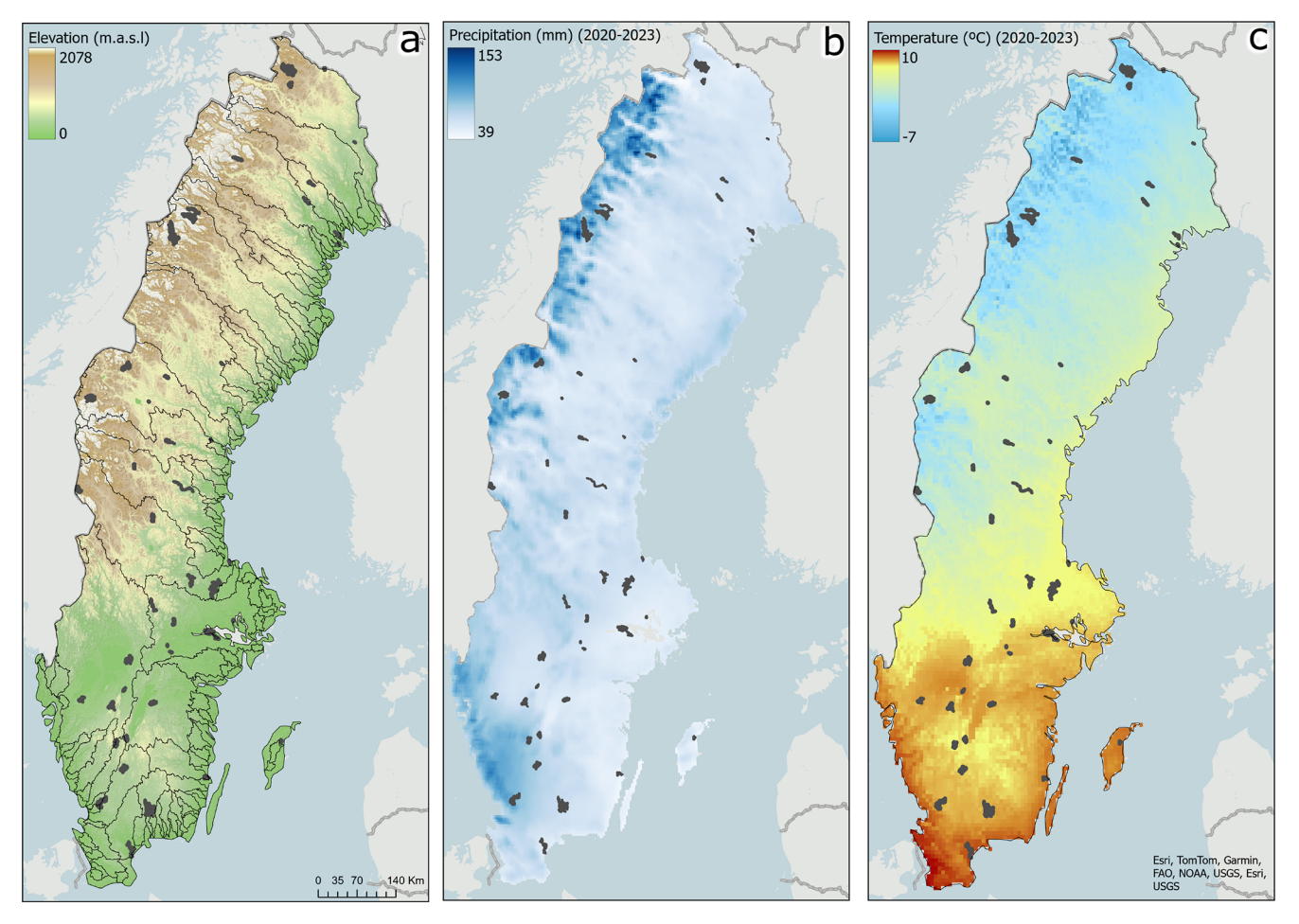


Figure 1. Spatial distribution of Ramsar wetland study sites (grey polygons) in terms of (a) elevation from a 50 m resolution DEM by Landmäteriet (grey thin lines denote main catchments), (b) average precipitation in mm/month between 2020 and 2023, and (c) average temperature in °C between 2020 and 2023. Temperature and precipitation data were obtained from the Precipitation Temperature Hydrological Agency's Water Model (PTHBV), available at the Swedish Meteorological and Hydrological Institute (SMHI).

eation was performed by an interpreter experienced in SAR imagery analysis and conducted blind (without prior exposure to DeepAqua predictions). For the second approach, we assess the accuracy of the predicted hydrological regimes by comparing them to daily discharge data from nearby active stations provided by the Global Runoff Data Centre (GRDC, 2025) and SMHI (2025). In total, there were 23 sites with available discharge data either upstream, downstream, or onsite of the wetland. For both approaches, we calculate the error between the DeepAqua predictions compared to (1) manually delineated water extent and (2) daily discharge using the normalized root mean square error (NRMSE). We normalize the root mean square error (RMSE) to the range of water extent to discount the total area from the error result and to make each wetland comparable with the others.

2.4 Cluster analysis

The hydrological regimes based on DeepAqua's water extent predictions (Sect. 2.3) were clustered based on their hydrological similarity using a multivariate K-means cluster analysis technique and means of visual interpretation. K-means clustering is a widely used and simple unsupervised machine learning technique in which groups are identified based on the Euclidean distance between a data point and a centroid (a mean of the data) (Everitt et al., 2011). To ensure reproducibility, we set the random seed to 42, preventing variations in the clustering results between runs. In order to conduct a cluster analysis, data points that characterize the hydrological regime given by water extent are required. We calculated several hydrological parameters based on each hydrological regime and used them as the input data points (Table A1). The hydrological parameters included known hydrological signatures (Olden and Poff, 2003) and custom parameters to describe the hydrological regime in terms of duration, timing, frequency, magnitude, and rate of change. The optimal number of clusters (k) was chosen based on the inflection point on the elbow curve, which calculates the withincluster sum of squares (WCSS) for a range of cluster sizes from 1 to n. The inflection point on the elbow curve is interpreted at the optimum number of clusters since it indicates the point where adding more clusters results in a diminishing reduction in WCSS. The best-performing parameters were picked using visual inspection (inspecting their ability to cluster the regimes) and validated against multicollinearity using the variance inflation factor (VIF). The VIF measures the degree of multicollinearity of one hydrological parameter with all other parameters by calculating how much the variance of the regression coefficient increases due to correlation with other independent variables. We recognize that there is some degree of inherent correlation between the hydrological parameters since they are descriptors of the same hydrological regime. Therefore, we used a VIF value of <10 as an indicator that the hydrological parameters were not highly multicollinear and did not describe the same regime characteristic (Fig. 5a).

The emerging pattern given by the elbow curve indicated that individual hydrological regimes among wetlands were best grouped when k=4–6 (Fig. A1). Upon visual inspection, k=5 was chosen as the best possible distribution of wetlands into roughly equal-sized groups. The number of sites in each cluster ranged between 6 and 15. Each hydrological parameter was tested individually and in combination with other parameters to see how effectively they helped cluster the wetlands. Certain variables, such as the maximum month, dominated the clustering over other indices, and some index pairs were extremely collinear, such as maximum month and minimum month or spring/summer slope difference and slope variation. Therefore, these pairs could not be used together for the final clustering analysis.

3 Results and analysis

3.1 Surface water extent validation

When comparing water extent predictions from DeepAqua to manually delineated water extent to a systematic sample of wetlands, we find that predicted water extent performs well with their manually delineated counterparts (Fig. 2). Hjälstaviken and Dättern wetlands had the lowest NRMSE with 0.04 and 0.07, respectively, whereas the Maanavuoma wetland exhibited the highest error between the manually delineated water extent and the DeepAqua prediction with an NRMSE of 0.12. The majority of error between the DeepAqua and the manual water extent estimates originates from the spring and autumn months for many of the sampled wetlands. This is particularly apparent in Maanavuoma and Tysöarna wetlands. In both cases, the water extent is underestimated by DeepAqua compared to the manual esti-

mate. In the Store mosse wetland, DeepAqua tends to overestimate wetland water extent compared to when the water extent is manually delineated. Overall, all five sampled sites have strong agreement in the shape and magnitude of the hydrological regime, indicating that DeepAqua captures the seasonal hydrological characteristics with good accuracy (Fig. 2f).

To enhance the strength of our validation approach, we compared the wetland hydrological regimes to in situ daily discharge measurements (Fig. 3). Among the 23 wetlands with available discharge data, three had an active gauging station located upstream, two had on-site stations, and 16 had stations situated downstream (Fig. 3a). Of these, eight sites featured regulatory structures (e.g. dams, weirs, or culverts) along their river courses, which may disrupt the natural flow regime and weaken the correlation between wetland water surface extent and stream discharge. In general, stations with lower mean discharge returned lower NRMSE values between water extent and discharge (Fig. 3b). However, the relationship is weak ($R^2 = 0.17$) and based on a limited number of observations (n = 23). Most sites cluster in the bottom-left portion of the plot, with a few high-discharge, high-NRMSE outliers in the top right. Regulated and nonregulated sites are distributed throughout, with no strong visual separation, although none of the regulated sites exhibit low discharge and low NRMSE values.

Figure 4 presents a sample of wetlands with unregulated flow between discharge stations located either upstream or downstream. In general, daily discharge replicates the shape of the wetland's hydrological regime. The correlation between river discharge and wetland hydrological regime is particularly apparent for Tjålmejaure-Laisdalen (NRMSE 39.49), Östen (NRMSE 31.40), and Helge å (NRMSE 12.70) wetlands, whereby increased discharge matches increased water extent well in the spring months, followed by relatively reduced flow thereafter.

Although Tjålmejaure-Laisdalen and its corresponding downstream station are separated by $\sim 116\,\mathrm{km}$ of watercourses, the discharge data agree well with the wetland water extent. For the Maanavuoma wetland (NRMSE 0.92), data from the discharge station situated $\sim 15\,\mathrm{km}$ upstream agree with water surface extent in 2020 and 2021. However, the spring surge of water in 2022 and 2023 that is present in the river is not experienced by the wetland. Lastly, they also agree well in the Storkölen wetland (NRMSE 9.37) despite greater interannual variability compared to other sites. Notably, both time series show a pronounced peak between April and May 2021, reflecting a concurrent increase in wetland water extent.

3.2 Cluster analysis

Based on the surface water extent data, we conducted a K-means cluster analysis to explore patterns in the shape and characteristics of wetland hydrological regimes. Of all

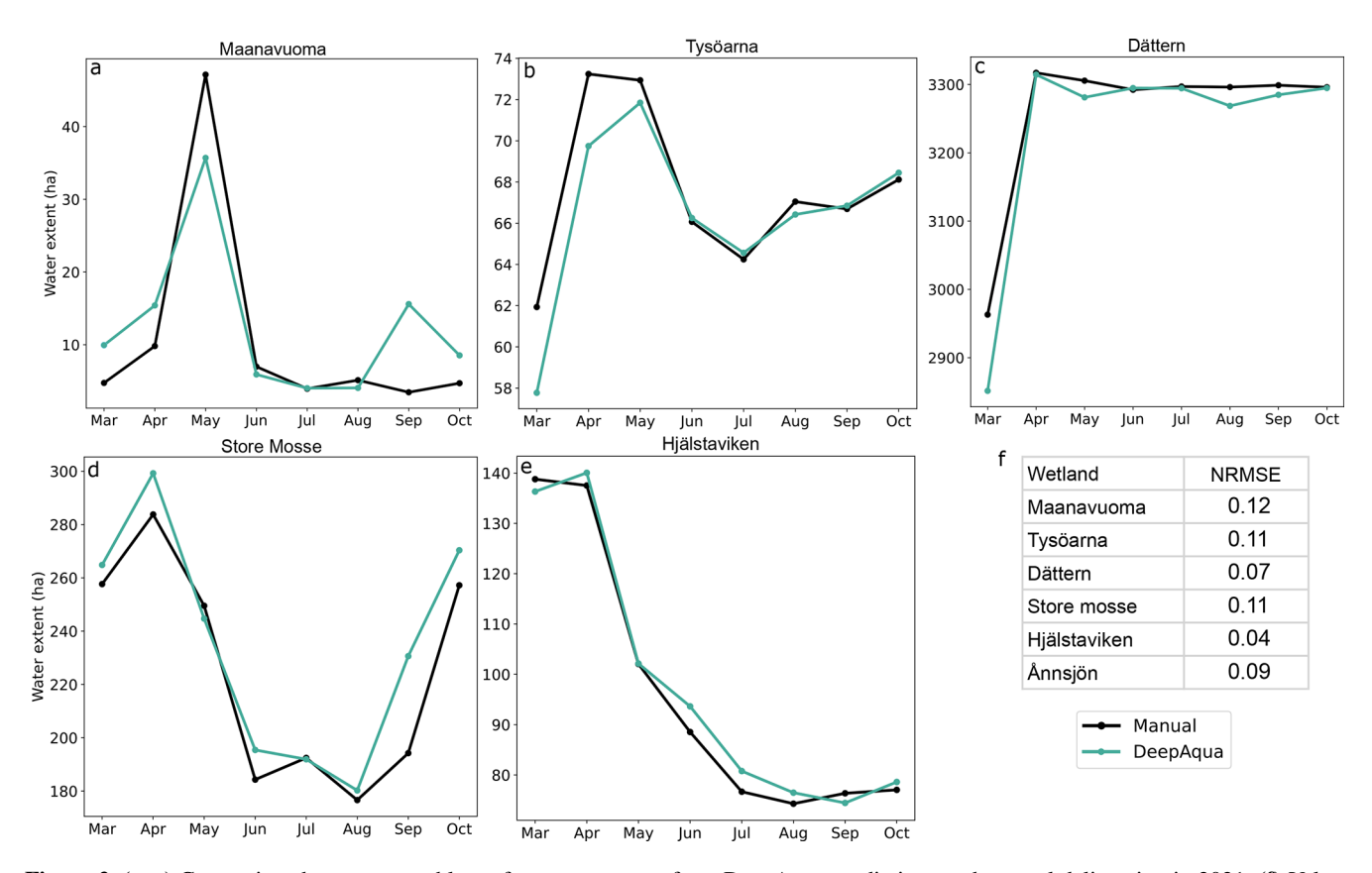


Figure 2. (a–e) Comparison between monthly surface water extent from DeepAqua predictions and manual delineation in 2021. (f) Values of normalized root mean square error (NRMSE; RSME divided by the range in wetland extent) between manually delineated and DeepAqua predictions.

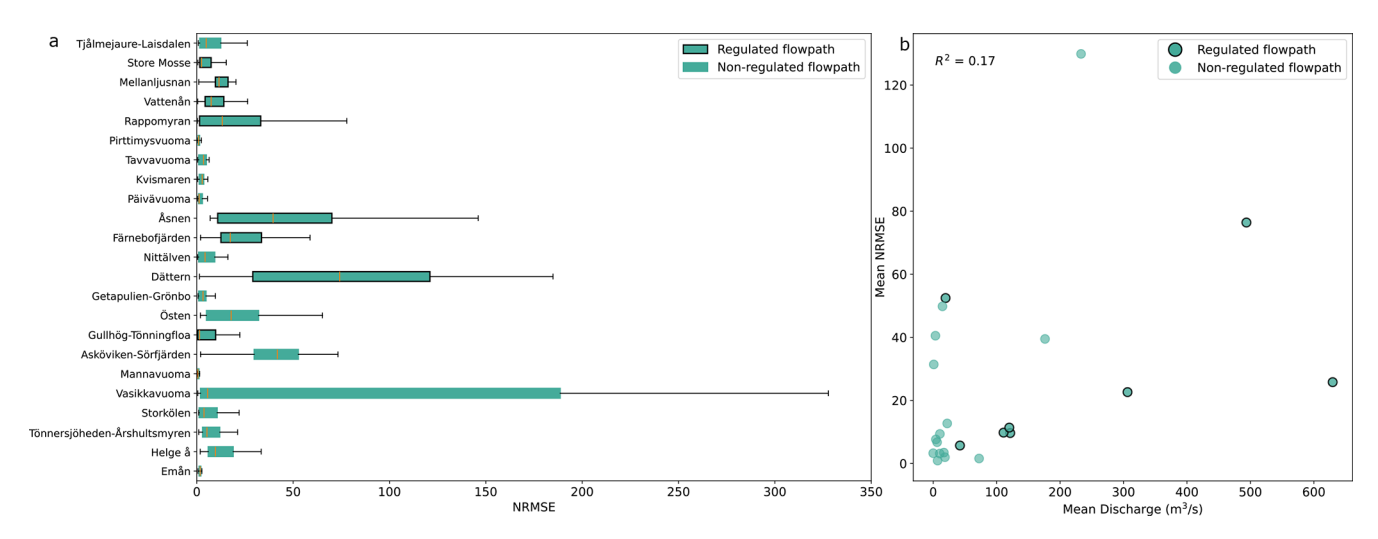


Figure 3. (a) NRMSE between daily discharge and wetland water extent for the 23 wetlands with available discharge data. Green boxes indicate the interquartile range (IQR), whiskers represent the range, and orange lines show the mean NRMSE. **(b)** Mean NRMSE versus mean discharge for each wetland, calculated over matching dates from January 2020 to August 2023. Wetlands with regulated flow paths between the wetland pour point(s) and discharge station are indicated by black outlines.

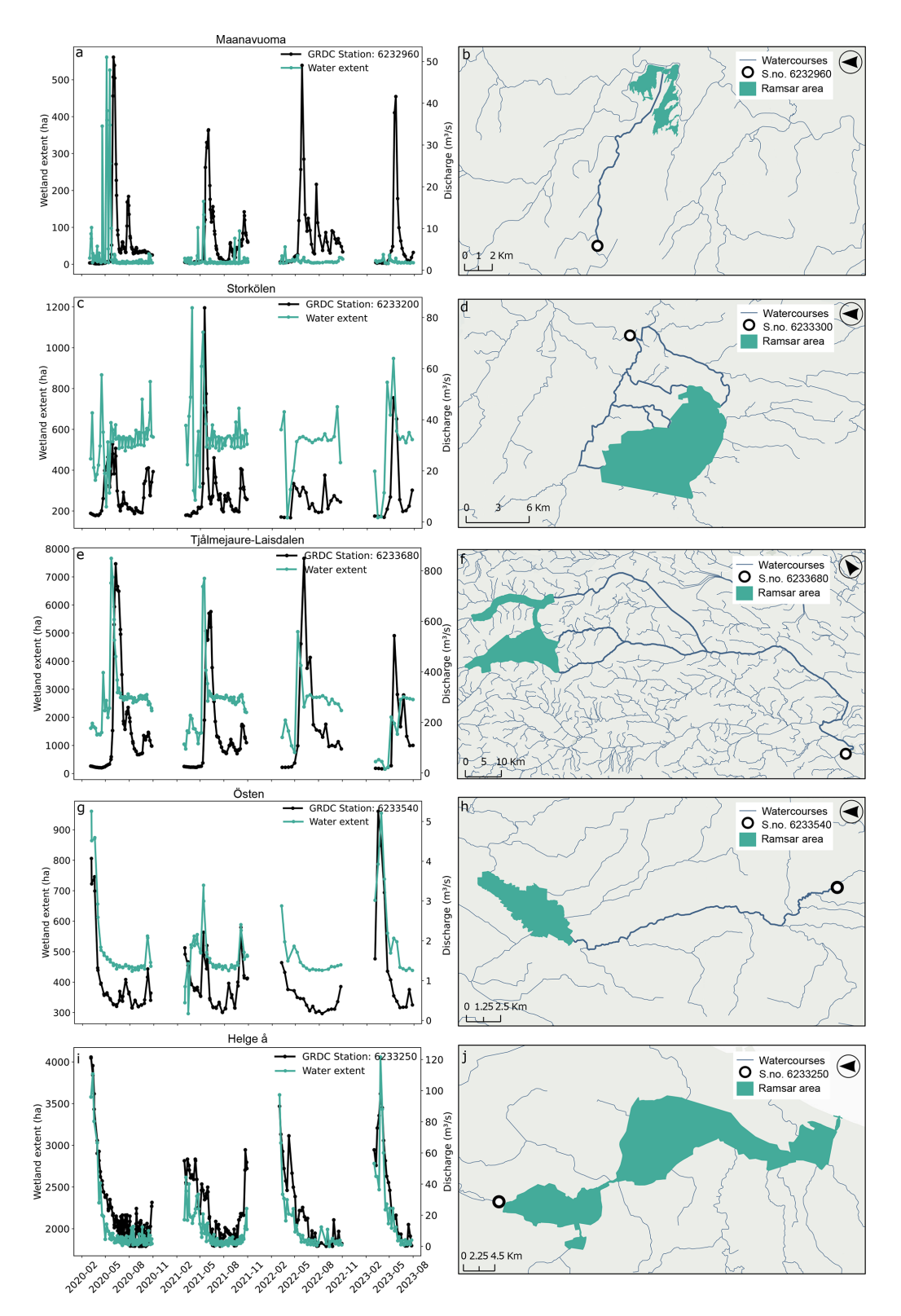


Figure 4. Left panel: comparison of water surface extent and discharge from on-site, upstream, or downstream stations for corresponding dates in Maanavuoma, Storkölen, Tjålmejaure-Laisdalen, Östen, and Helge å wetlands from January 2020 to August 2023 (excluding winter months). The GRDC station IDs are shown in the upper left of each plot. Right panel: wetland boundaries (green polygons) as defined by the Ramsar Convention, with discharge stations (black rings), watercourses between the station and wetland (thick blue), and other watercourses (thin blue).

parameters assessed, skewness, kurtosis, normalized maximum slope, number of peaks, and baseline month fraction (Fig. 5a) were found to collectively capture key regime characteristics (Fig. 5b). Upon visual inspection, regimes with similar shapes were grouped together while also maintaining the desired VIF condition (<10) with values of 3.96, 1.60, 4.07, 3.01, and 6.54 for skewness, kurtosis, maximum slope, number of peaks, and baseline month fraction, respectively. These values indicate a reasonable level of nonmulticollinearity between all other variables. The chosen parameter combination successfully clusters related hydrological regimes into five different archetypes, with the number of sites (n) in each archetype as follows: "spring-surging" (n = 6), "spring-flooded" (n = 8), "summer-flooded" (n =8), "slow-drying" (n = 15), and "summer-dry" (n = 6). Support for the archetype names is given by the hydrological parameter results, which have been averaged by archetype and are described in Sect. 3.3.

3.3 Hydrological archetype analysis

The overall spatial distribution of the archetypes and thematic graphic descriptions of the hydrological regime given by water surface extent are presented in Fig. 6. The springsurging wetlands (Fig. 6a) are only found in northern Sweden and have flashy hydrological regimes, consisting of a dry baseline condition and a brief period of increased water extent. Spring-flooded wetlands (Fig. 6b) are limited to southern and central Sweden. The hydrological regime of these wetlands resembles that of spring-surging wetlands, although they have a relatively longer spring peak. Summerflooded wetlands (Fig. 6c) remain inundated from May to October after a rapid wetting period and are spread across Sweden. Southern Sweden's slow-drying wetlands (Fig. 6d) exhibit steadily decreasing water extent throughout the summer, reaching minimum water extent in autumn. Lastly, summer-dry wetlands (Fig. 6e) exhibit the maximum wetland extent in April, preceding generally dry conditions until September-October.

One of the most distinctive differences between archetypes is the magnitude of water extent at the beginning of spring. For instance, slow-drying and summer-dry archetypes already have large water extents in March and, therefore, do not undergo a rapidly inundating period during spring or summer. The lack of any inundation period is reflected in the normalized maximum slope values (Fig. 5f, g), which are the lowest out of all archetypes, suggesting smaller changes in water extent across the year (0.21 and 0.14 for summer-dry and slow-drying, respectively). Additionally, archetypes with large water extent in spring tend to be found in central and southern Sweden, while archetypes such as spring-surging and summer-flooded wetlands start with a small water extent in March preceding a rapid inundation period. These archetypes, with higher normalized maximum slope values

of 0.59 and 0.77, respectively, are more abundant in the north (Fig. 5c, e).

A second defining feature between different archetypes is the duration of the dry period (baseline fraction), defined by months with water extent within the 25th percentile of the range. Archetypes with a significant dry period, such as summer-dry, spring-surging, and slow-drying wetlands, have high baseline month fractions (0.65, 0.63, and 0.66, respectively) and positive skewness (1.14, 1.45, and 1.58, respectively), which indicates that wet conditions are limited to the spring months (Fig. 5g, c, f). Conversely, with a negative skewness and low baseline month fraction (-1.60 and 0.17, respectively; Fig. 5e), summer-flooded wetlands are the only archetype that retains its large water extent throughout the year.

The resulting archetypes show how wetland hydrological regimes can be broadly differentiated into two primary "modes": peaky and smooth. We define peaky regimes as those with large fluctuations in water extent, while *smooth* regimes follow more consistent, gradual changes in monthly water extent. Peaky archetypes, such as spring-surging (Fig. 7a) and summer-flooded wetlands (Fig. 7c), exhibit relatively high values of kurtosis (2.27 and 2.93, respectively), maximum slope (0.59 and 0.77, respectively), and the number of peaks (1.2 and 1.0, respectively). On the other hand, smooth archetypes, like slow-drying and summer-dry wetlands, are characterized by relatively stable water extent from March to October (Fig. 7d, e). Spring-flooded wetlands share some traits with peaky archetypes, particularly a marked increase in water extent during spring (Fig. 7b) and high normalized slope values (0.70). However, they differ from typical spring-surging or summer-flooded wetlands in having a low average kurtosis (-0.04), which suggests a more even distribution of water extent over time. Although we refer to peaky archetypes here, it is important to note that the number of peaks is not necessarily descriptive of just peakedness (kurtosis). For instance, slow-drying wetlands have high kurtosis (2.03) yet few peaks on average (0.2), indicating that although they experience large variability in water extent, there is no distinguishable wet month.

Another approach to interpreting archetypes is by examining the degree of homogeneity within each archetype. This is because some archetypes share more similarities in terms of their environmental characteristics and hydrological regimes. For instance, summer-dry wetlands are mostly comprised of mires or open wetlands (Fig. 8d), typically lying at low elevations and exhibiting similar hydrological regimes (Fig. 7e). Spring-surging wetlands are also considered a homogenous archetype, since they are located primarily in high-latitude regions (Fig. 8a), are mainly fjäll wetlands, and tend to have little variability in their hydrological regime (Fig. 7a). In contrast, spring-flooded and summer-flooded wetlands are found all over Sweden across a range of elevations (Fig. 8b) and encompass many different wetland types. This highlights that hydrological regimes are not always associated

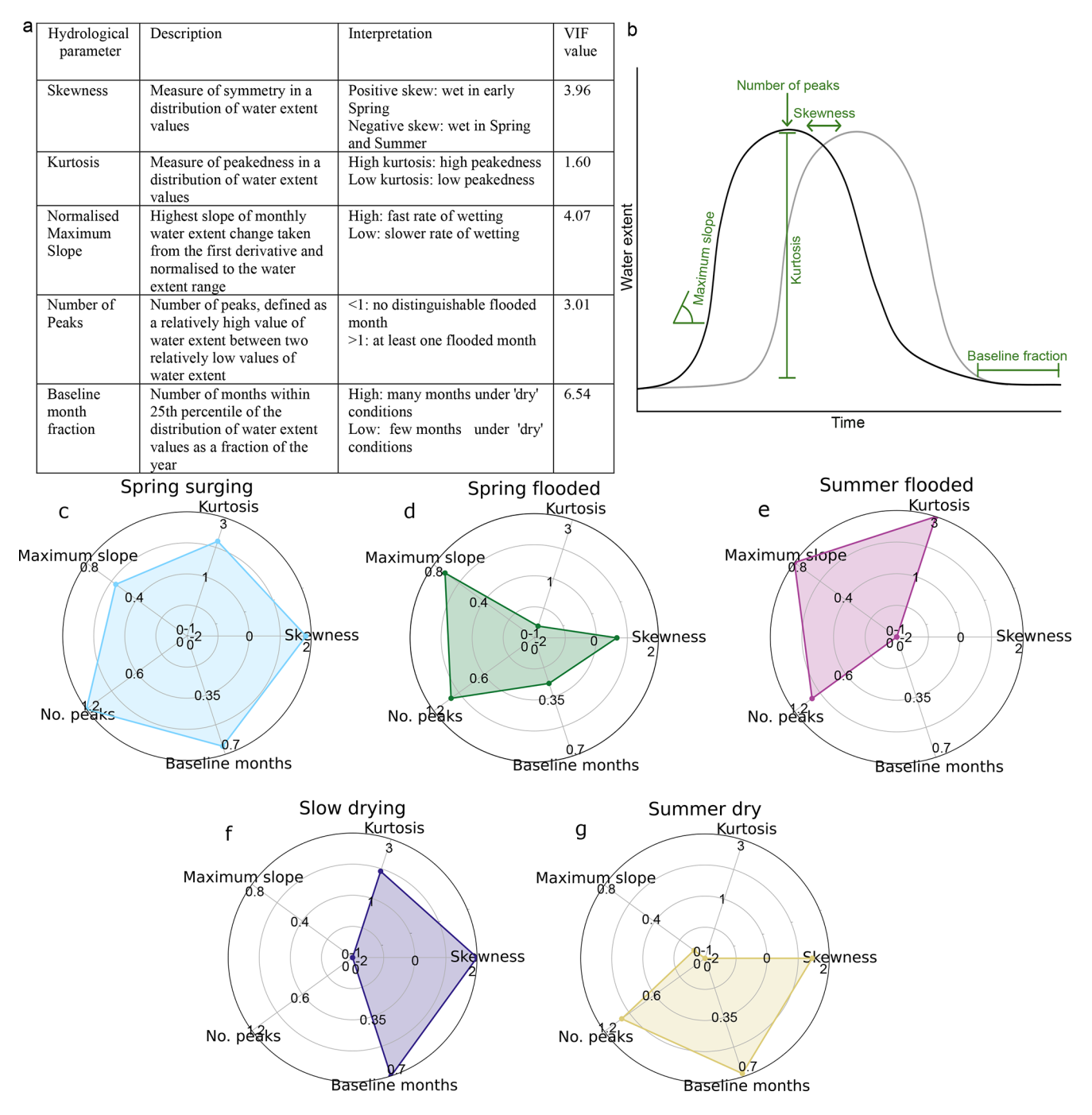


Figure 5. (a) Overview of the chosen parameter (unitless) combination used for the final cluster analysis of the hydrological regimes given by water extent and the VIF value for each parameter. (b) Graphical representation of the five selected hydrological parameters used to describe the characteristics of the hydrological regime for the final cluster analysis. (**c**–**g**) Radar plots for the final hydrological parameters averaged by archetype.

Figure 6. Spatial distribution of hydrological archetypes for sampled Ramsar wetlands in Sweden (n = 43) and representation of their hydrological regime through March and October. (a) Springsurging wetlands (n = 6), (b) spring-flooded wetlands (n = 8), (c) summer-flooded wetlands (n = 8), (d) slow-drying wetlands (n = 15), and (e) summer-dry wetlands (n = 6).

with a specific wetland type, but rather depend on the broader archetype to which the wetland belongs.

Despite the varying degrees of diversity within archetypes, grouping wetlands into archetypes still reveals a remarkable similarity in the timing of key features of their hydrological regimes. For instance, most summer-flooded wetlands reach low water extent by May or June, despite varying rates of drying for the rest of the year. This indicates that the hydrological parameters correctly capture timing characteristics, even across archetypes with more heterogeneity, such as summer-flooded wetlands.

A. E. Robinson: The hydrological archetypes of wetlands

4 Discussion

4.1 The value of archetypes for understanding wetland hydrology

One of the defining features for most archetypes was the timing of large changes in surface water extent, which only became apparent when the sites were grouped into archetypes. This highlights the usefulness of employing archetypes in hydrological studies, as hydrological regimes may not be best evaluated across sites when using a single parameter (Cutler and Breiman, 1994; Huggins et al., 2024; Piemontese et al., 2020). Although our classification was based solely on surface water dynamics, it also inevitably captured the cumulative effects of other environmental factors, such as vegetation, soil type, and climate. The archetype approach to classification is further supported by Bullock and Acreman (2003), who concluded that grouping wetlands based on their local classification term is less intuitive than grouping them by hydrological characteristics. This suggests that the hydrological perspective is a valuable lens for understanding ecosystem services of wetlands, especially when complemented with other environmental data (Okruszko et al., 2011; Poff et al., 1997).

4.2 Methodological considerations

Despite the overall success of the classification, not all wet-lands were easily categorized. We suggest that there are two main reasons for this. First, the hydrological regimes of some wetlands may form a continuum rather than falling into clearly separated categories, making strict archetype assignment challenging. Second, the limited scope of the wetland database used for clustering might have excluded the existence of additional archetypes that could emerge from a broader dataset. It is also important to note that our archetypes were defined from ~ 4 years of monthly water extent data, representing only the observed period. This relatively short-term record is unlikely to capture the full range of long-term hydrological variability. Longer observational periods are necessary for determining extended trends and assessing the impact of changing climatological conditions.

Our results were also shaped by the choice of sensor. Using water extent as our key measurement, SAR imagery provided dense spatiotemporal coverage across 43 wetland sites, which can be applied to any wetland larger than 200 ha. The reliance on remote sensing is driven by a lack of in situ data, which would have partly or wholly missed the hydrological regime signatures for most of the chosen wetlands in this study. However, this also limits the generalizability of our findings, since smaller wetlands may differ hydrologically and therefore may not conform to our archetype distribution. In addition, Sentinel-1 SAR has intrinsic limitations. C-band radar wavelengths likely underestimate surface water extent in wetlands, particularly under dense vegetation (Adeli et al.,

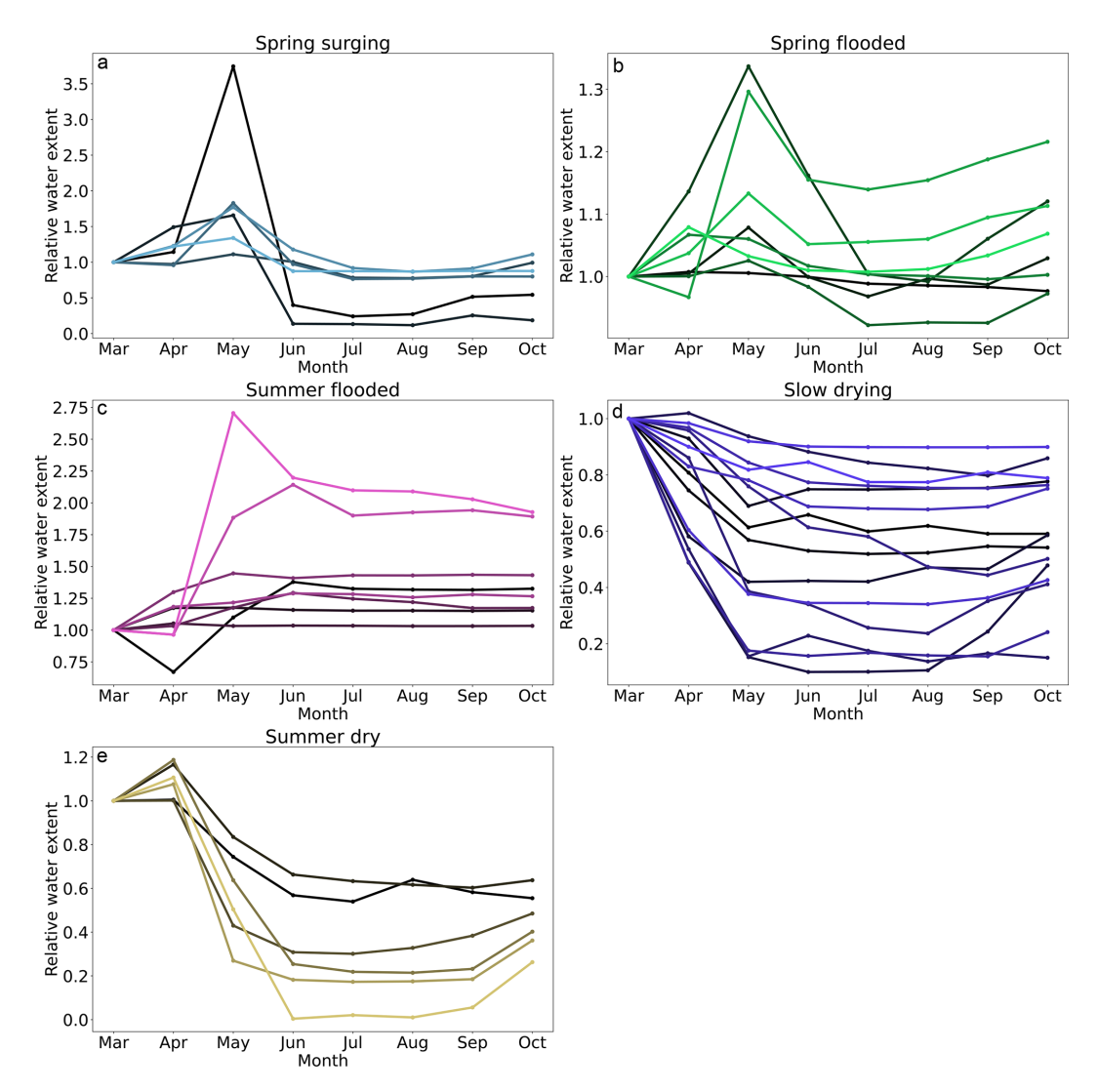


Figure 7. Hydrological regimes of individual wetlands per archetype based on a monthly average of surface water extent between January 2020 and August 2023. The water extent area for each month is shown relative to the water extent area in March.

2021). Surface water detection would therefore benefit from longer-wavelength radar, such as that on board the NISAR mission launched in July 2025.

To efficiently process large volumes of remotely sensed data, we chose an automatic deep-learning-based approach (DeepAqua) to detect water extent without the need for extensive manual annotation. However, DeepAqua was trained on a limited number of SAR scenes, and therefore it could only produce accurate predictions between January 2020 and August 2023. Future model development should aim for greater temporal generalizability and reduced sensitivity to changes in Sentinel-1 backscatter distributions, enabling the use of the >10 years of Sentinel-1 data currently available.

An additional assumption of our study is that surface water extent is analogous to total water storage, which may not be true for mire types (Acreman and Holden, 2013) or topographically constrained wetlands. Therefore, including

water level data from hydrogeodetic technologies such as the Surface Water and Ocean Topography (SWOT) mission (Hamoudzadeh et al., 2024) or soil moisture observations (Mupepi et al., 2024) could improve hydrological regime classification, especially for seasonal wetlands (see more examples in Jaramillo et al., 2024).

Finally, other hydrological variables could improve the explanatory power of the archetypes. Snow and ice interfere with SAR-based water detection methods, which leave winter hydrology poorly observed. Limited availability of discharge stations further restricts observational validation. Incorporating additional data such as groundwater inputs, evapotranspiration, and hydrological connectivity metrics could provide a more complete picture of wetland hydrology.

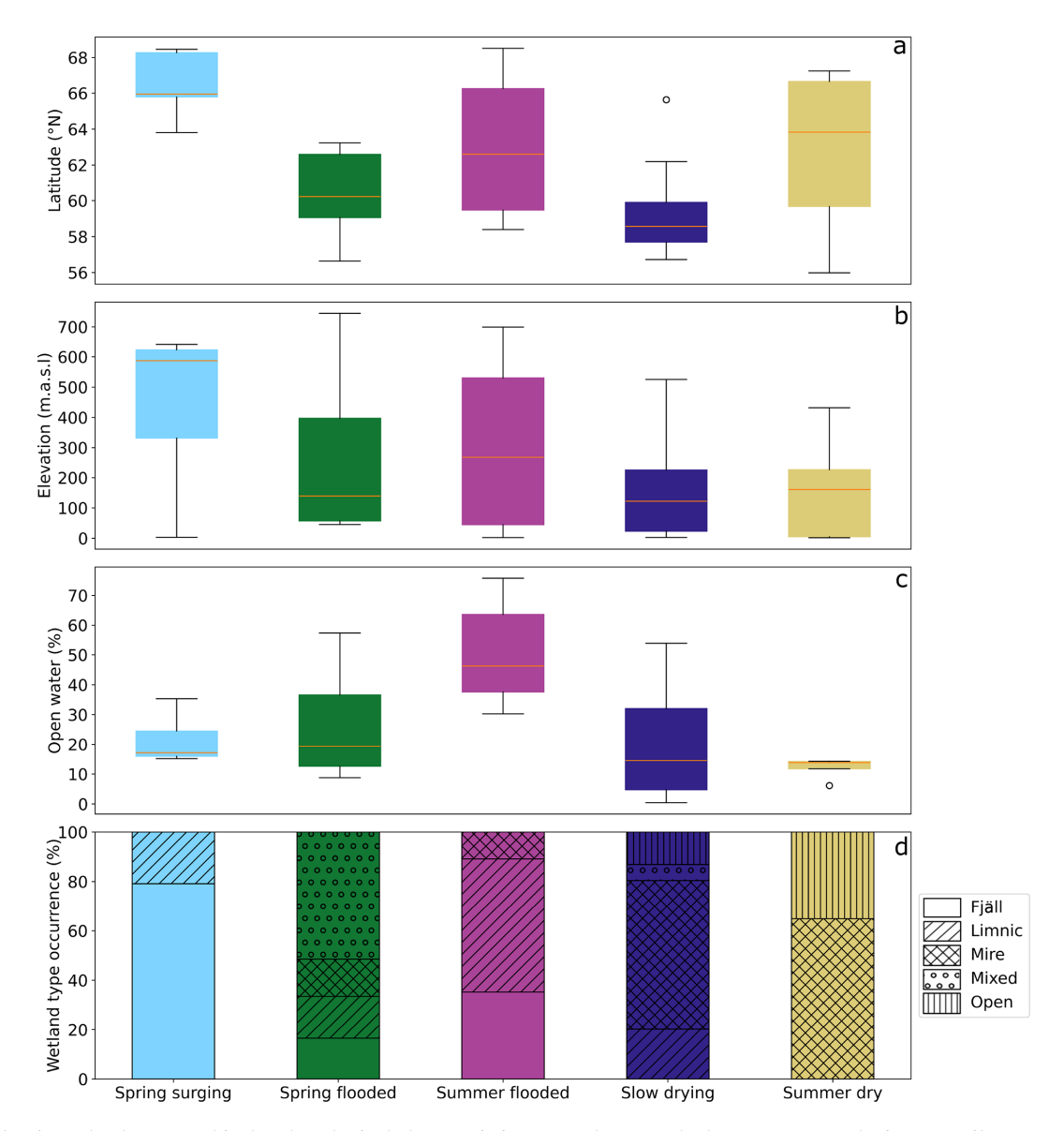


Figure 8. (a–c) Wetland topographical and ecological characteristics per archetype. The boxes represent the interquartile range (IQR), with orange lines indicating the mean value across all wetlands within each archetype. Whiskers outline the range, and small black circles denote wetlands with anomalous results compared to the rest of the archetype. (d) Stacked bar plot showing the occurrence of wetland types (fjäll, limnic, mire, mixed, or open) per cluster as a percentage of the total number of sites in each archetype.

4.3 Controls and variability in wetland hydrological behaviour

Although detailed exploration of the physical drivers of the observed hydrological regimes is beyond this study's scope, we theorize that factors such as position within the watershed and surface connectivity contribute at least to some extent. For example, spring-surging wetlands, with few surface water inlets, rely mainly on snowmelt and tend to dry rapidly, while summer-flooded wetlands benefit from multiple inflows and sustain inundation longer (Lane et al., 2018). Secondly, wetlands located in headwater regions, like spring-surging and summer-flooded wetlands, experi-

ence rapid flood peaks characteristic of upper catchment water flows. This is in contrast to wetlands such as those within the slow-drying archetype, which are located in the lower parts of the catchment and are therefore linked to less pronounced flood peaks (Morley et al., 2011). Similar seasonal patterns have been described for downstream wetlands in climates with high winter precipitation, where water levels remain high from November to April before declining during summer and rising again at the onset of the wet season (Lane et al., 2018). These dynamics also correspond to the winter-rainfall catchments in Sweden identified by Matti et

al. (2017), which generally experience flood peaks early in the year and/or after autumn.

It should also be acknowledged that hydroclimatic variability plays a critical role in shaping wetland hydrological regimes and represents an important consideration for the interpretation of our archetypes. On interannual and seasonal timescales, fluctuations in precipitation, snowmelt, and evapotranspiration strongly influence wetland hydroperiods (Jaramillo et al., 2018; Winter, 2000). For instance, snowaffected wetlandscapes typically reach maximum inundation extent later in spring – similar to our spring-surging wetlands, while rain-fed wetlandscapes peak earlier in the year, closely resembling the regime of slow-drying wetlands (Park et al., 2022). Latitudinal gradients in inundation duration, with shorter hydroperiods in northern Sweden and longer ones in the south (Prigent et al., 2001), broadly align with our results.

On a climatic temporal scale, warming trends and an increasing dryness index have been observed in Swedish wetlandscapes since the 1970s, suggesting that there is a greater evaporative demand and reduced water storage in wetlands, especially during summer (Åhlén et al., 2021). These observations also align with model projections showing substantial summer drying and reduced wetland extent in North America under high-emission scenarios due to evapotranspiration exceeding precipitation input (Xu et al., 2024). Similarly, Xi et al. (2021) projected future declines in inland wetland area across Europe, though with a higher degree of uncertainty in Scandinavia. Furthermore, hydrological stability will likely be reduced in the future, with modelled studies of prairie pothole wetlands showing diminished monthly-scale stability in water storage under uncertain climate conditions (Zhang et al., 2011).

Despite this, the degree to which wetlands are vulnerable to such changes is dependent on their dominant water sources and topographical setting. For example, wetlands that are reliant on direct precipitation or snowmelt, such as spring-surging wetlands, are more sensitive to hydroclimatic variability, while wetlands sustained by regional groundwater inputs on larger floodplains (like slow-drying or spring-flooded wetlands) have greater buffering capacity to hydroclimatic change (Winter, 2000). These findings highlight the need for long-term observations and the integration of hydroclimatic data when interpreting wetland hydrology in future work.

4.4 Hydrological regimes as indications of ecosystem services

In this study, we quantified the hydrological regimes of Swedish wetlands to better understand their hydrological functions, which are closely tied to the ecosystem services they provide. Inland wetlands are estimated to contribute approximately Int\$ 27 trillion annually in ecosystem service value, with the majority of the value deriving from water regulating services (Davidson et al., 2019).

We theorize that hydrological regimes can serve as indicators of the hydrological ecosystem services a wetland may deliver at any given time. For instance, spring-surging wetlands, which are characterized by high water extent during spring and low extent during summer, resemble headwater wetlands, which are known to increase high water flows during the wet season while retaining baseflow during the dry season (Bullock and Acreman, 2003). This suggests they may contribute less to flood mitigation and, in some cases, exacerbate flooding (Åhlén et al., 2022), a pattern supported by the Ramsar site descriptions, where no wetlands in the spring-surging archetype list flood control as a key service. Similar observations have also been made in wetlandrich headwater catchments in central Europe, which exhibit rapid activation of pre-event water, indicating an ability to quickly mobilize floodwaters (Votrubova et al., 2017). Nevertheless, headwater wetlands can provide temporary flood storage (Kadykalo and Findlay, 2016), but confirming such dynamics requires temporally dense water extent observations to capture lag times between water storage and downstream flows.

Conversely, slow-drying wetlands exhibit traits more typical of floodplain wetlands, which are well-documented in their role in flood reduction and water retention (Acreman and Holden, 2013; Golden et al., 2021; Opperman et al., 2010). The gradual reduction of water extent in these wetlands may suggest sustained water storage, likely contributing to both flood peak attenuation and maintaining summer baseflows. This aligns with Åhlén et al. (2022), who suggest that downstream wetlands in central Sweden remain relatively dry during summer while maintaining high buffering capacity. The Ramsar site descriptions for slow-drying wetlands further support this, since the majority of them have flood control and/or water storage listed as a known ecosystem service. Additionally, Doherty et al. (2014) suggest that wetlands with periodically dry soils (such as slow-drying or summer-dry wetlands) slow down flows and can remove large volumes of water from the system. Although we did not perform a detailed analysis of ecosystem service delivery or have dense downstream discharge data (Andersson, 2012), our results offer a foundation for prioritizing wetlands for future conservation or Ramsar designation, particularly in flood-prone or drought-prone regions.

Another strength of hydrological regime classification is its ability to infer hydrological functions at different times of the year, recognizing that wetland functions are not static in time or space (Spence et al., 2011). For example, variability in water extent can signal the transition between water storage and runoff-dominated states (Yanfeng and Guangxin, 2021). Flashy water extent variability observed in springsurging, spring-flooded, and to a lesser extent summerflooded wetlands suggests a switch to conditions where wetlands act as conduits rather than reservoirs. This may result from frozen ground hindering water storage in soils (Yanfeng and Guangxin, 2021) or the dominance of rapid snowmelt

inputs (Spence et al., 2011). However, further investigation combining water level, connectivity analyses, and catchment precipitation data would be needed to verify these hypotheses.

Aside from hydrological-related ecosystem services, wetlands offer other valuable ecosystem services that are also linked to their hydrological regimes, such as biodiversity and carbon sequestration (Okruszko et al., 2011). Hydrological variability is a major driver of wetland biodiversity due to species' water tolerance thresholds. Additionally, wetlands classified under the "northern" archetypes are particularly significant carbon sinks, as evidenced in Ramsar site records. Differentiating hydrological regimes in carbon-sequestering wetlands or those with particularly rich biodiversity could improve our understanding of their role in the delivery of other ecosystem services (Kirpotin et al., 2011).

5 Conclusion

This research aimed to improve our understanding of wetlands by revealing their hydrological regimes using remotely sensed observations of water surface extent. We chose an automatic detection method based on Sentinel-1 SAR imagery because it can operate in cloudy and dark conditions and detect more water under vegetation compared to optical-based methods. The hydrological regimes were grouped based on similar hydrological characteristics identified by custom hydrological parameters. For 43 Ramsar sites in Sweden, the hydrological regimes based on monthly water extent between 2020 and 2023 could be grouped into five distinct archetypes. The defining traits were mainly related to the timing of change and the duration of wet and dry periods. Despite heterogeneity in the archetypes' spatial distribution, flashy archetypes with high water extent variability were preferentially found at higher elevations and latitudes, while less variable and drier archetypes were concentrated towards low elevations and latitudes. Additionally, wetlands with mire types were more likely to be part of the same archetype compared to open or limnic wetland types.

While contextual information is vital for our deeper understanding of wetlands, valuable insights into runoff and storage dynamics can be gained simply by tracking water extent over time. Furthermore, by reducing multiple wetland hydrological characteristics to the hydrological regime, we demonstrated that we could use the concept of archetypes to infer information about their specific hydrological functionality nationwide. Since many archetypes consist of multiple wetland classifications, we recommend estimating hydrological functions based on the hydrological regimes, not individual wetland types. By being able to draw information from the archetypes, we reveal a new understanding of the hydrological functioning of wetlands with a particular emphasis on hydrological-related ecosystem regulating services such as flood control and water supply during low flow periods.

Appendix A

Table A1. Hydrological parameters used for cluster analysis. Each parameter was evaluated individually and in combination with others to assess its effectiveness in capturing the characteristics of the hydrological regime. (N) – normalized to remove the effect of wetland size.

Hydrological parameters	Description
Max month	Timing of the highest water extent
Min month	Timing of the lowest water extent
Standard deviation	Measure of dispersion of water extent values in a dataset
Skewness	Measure of symmetry in a distribution of water extent values
Kurtosis	Measure of peakedness in a distribution of water extent values
Coefficient of variation	Measure of the dispersion water extent values around the mean
Range (N)	Difference between the maximum water extent value and the minimum water extent value, normalized to the mean wetland size
Minimum slope (N)	Smallest slope of monthly water extent change taken from the first derivative, normalized to the water extent range
Maximum slope (N)	Highest slope of monthly water extent change taken from the first derivative and normalized to the water extent range
Spring/summer area difference (N)	Difference between the average spring water extent (in March, April, and May) and average summer water extent (June, July, August), normalized to the mean wetland size
Spring/summer slope difference (N)	Difference between the average spring slope of monthly water extent change (in March, April, and May) and average summer slope of monthly water extent change (June, July, and August), normalized to the mean wetland size
Slope variation (N)	Standard deviation of all month-to-month slopes of monthly water extent change, normalized to the water extent range
Number of peaks	Number of peaks, defined as a relatively high value of water extent between two relatively low values of water extent
Baseline month fraction	Number of months within 25th percentile of the distribution of water extent values as a fraction of the year

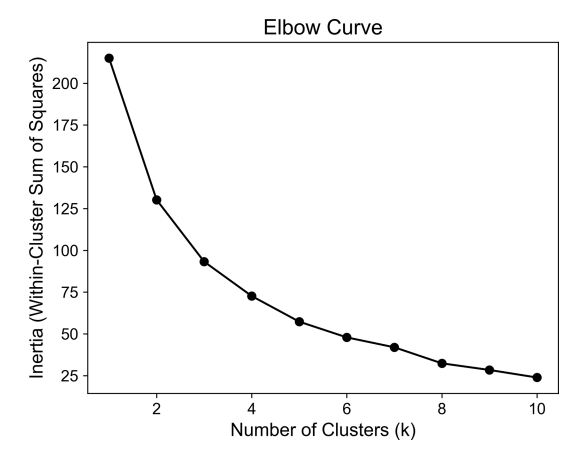


Figure A1. Elbow curve showing the within-cluster sum of squares (WCSS) for k values ranging from 1–10. The elbow curve helps identify the number of clusters by indicating where adding more clusters results in a diminishing reduction in the WCSS.

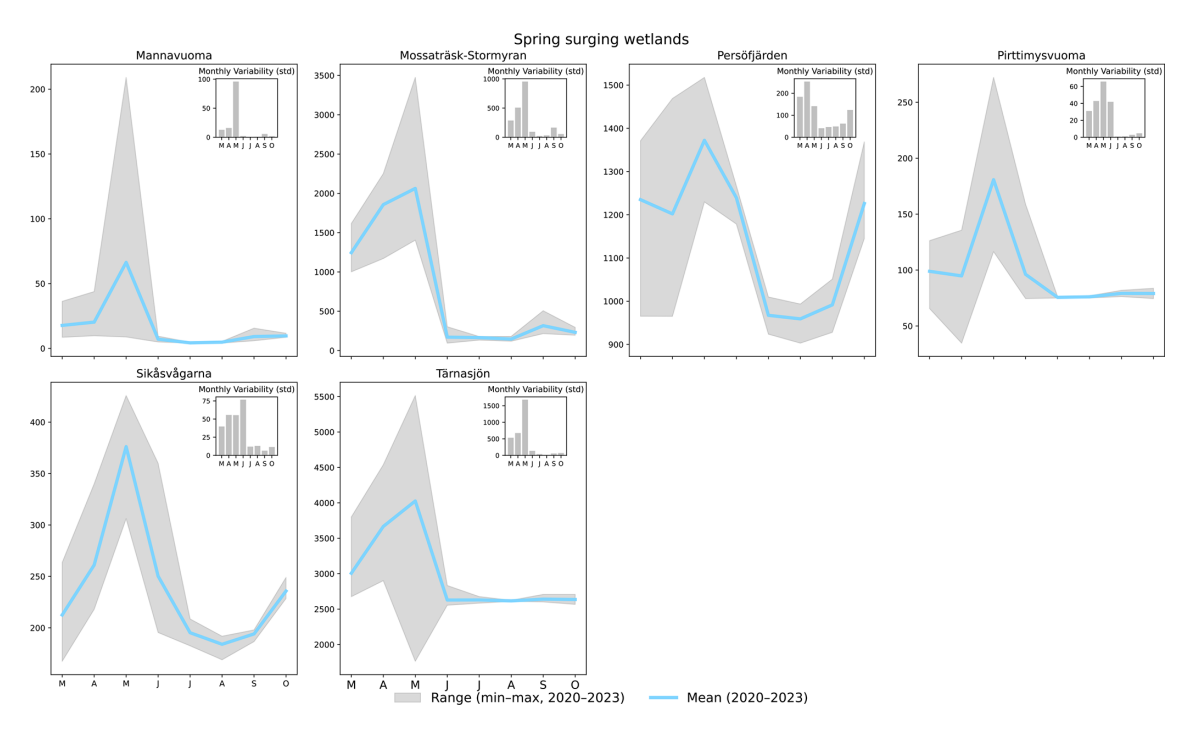


Figure A2. Average monthly water extent (March–October) between 2020–2023 for all wetlands belonging to the spring-surging archetype. Grey area shows the monthly interannual variability given by the range of water extent from all years. The monthly standard deviation is given in the top-right bar plots.

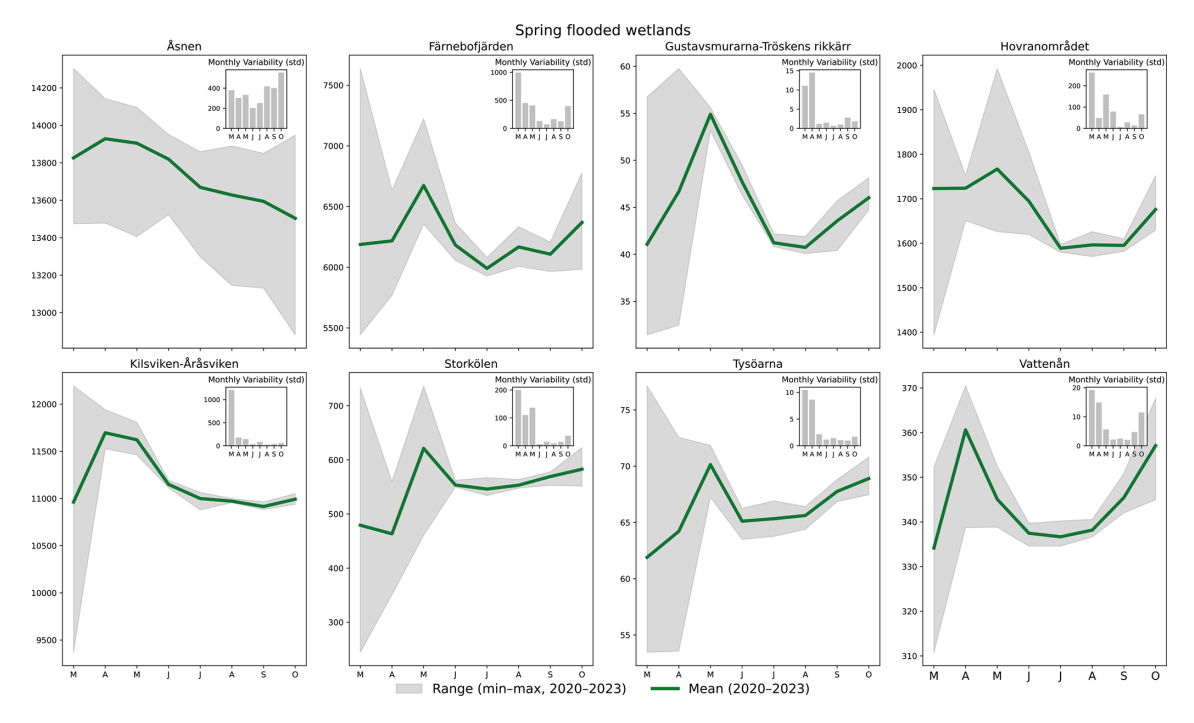


Figure A3. Average monthly water extent (March–October) between 2020–2023 for all wetlands belonging to the spring-flooded archetype. Grey area shows the monthly interannual variability given by the range of water extent from all years. The monthly standard deviation is given in the top-right bar plots.

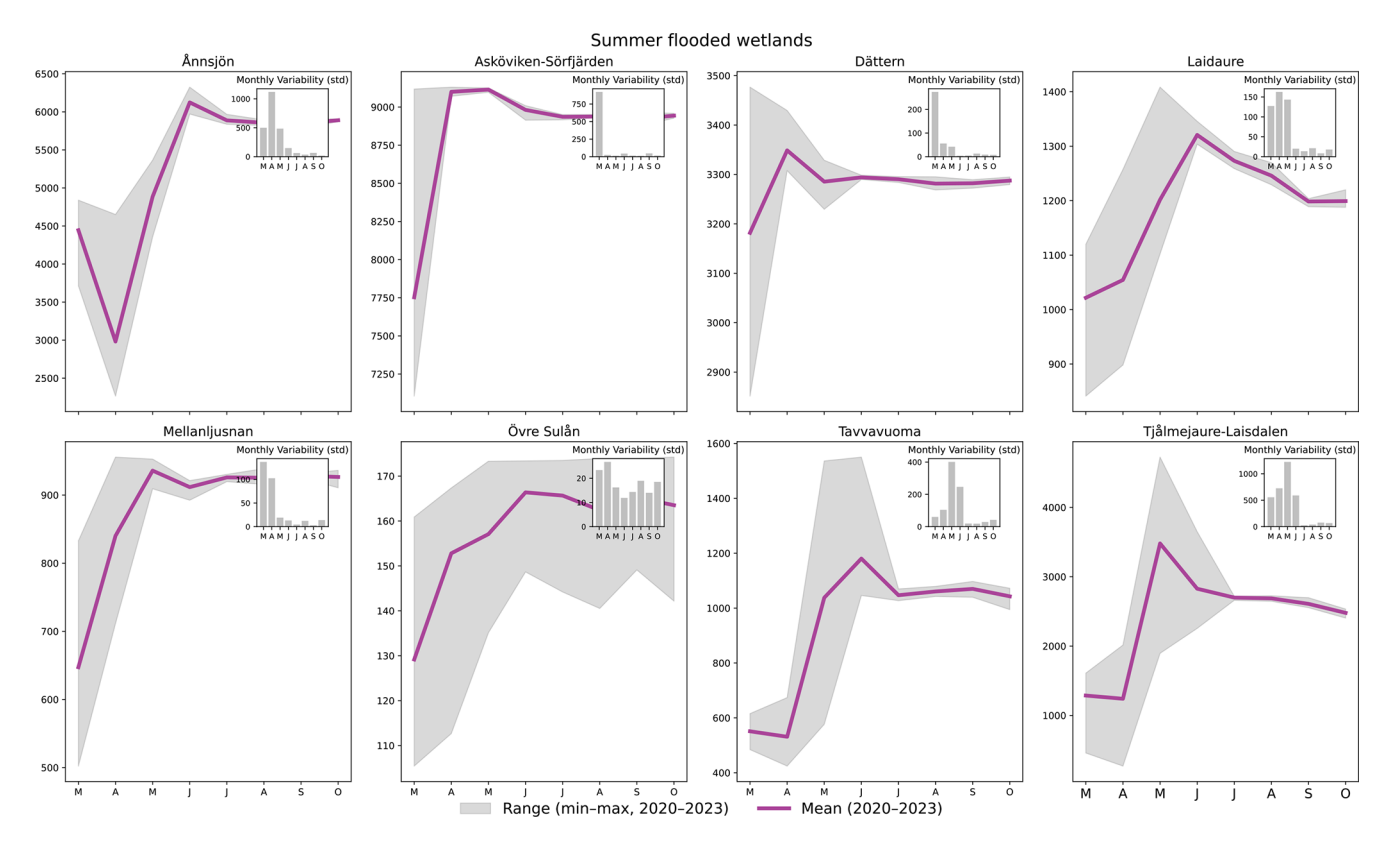


Figure A4. Average monthly water extent (March–October) between 2020–2023 for all wetlands belonging to the summer-flooded archetype. Grey area shows the monthly interannual variability given by the range of water extent from all years. The monthly standard deviation is given in the top-right bar plots.

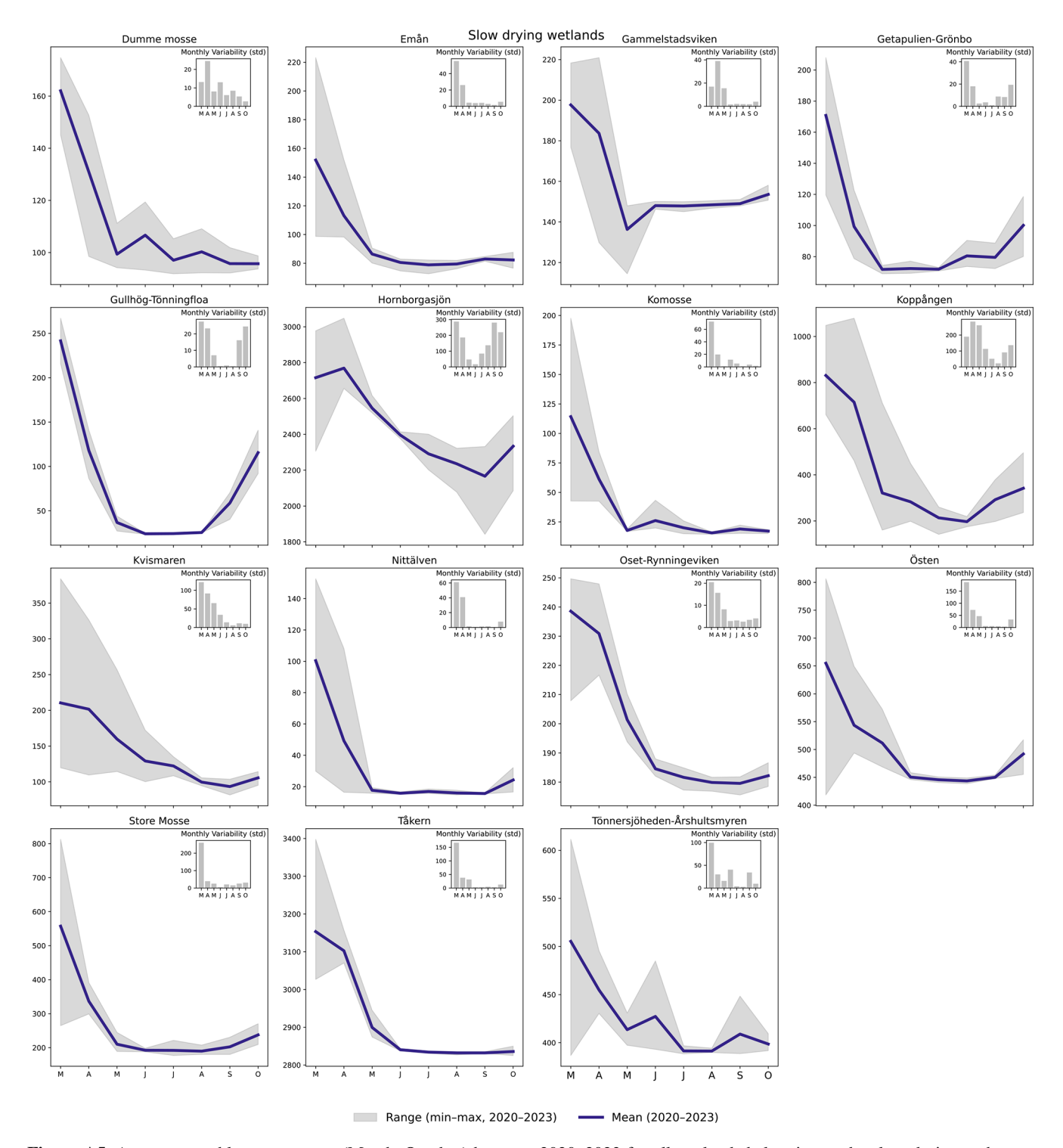


Figure A5. Average monthly water extent (March–October) between 2020–2023 for all wetlands belonging to the slow-drying archetype. Grey area shows the monthly interannual variability given by the range of water extent from all years. The monthly standard deviation is given in the top-right bar plots.

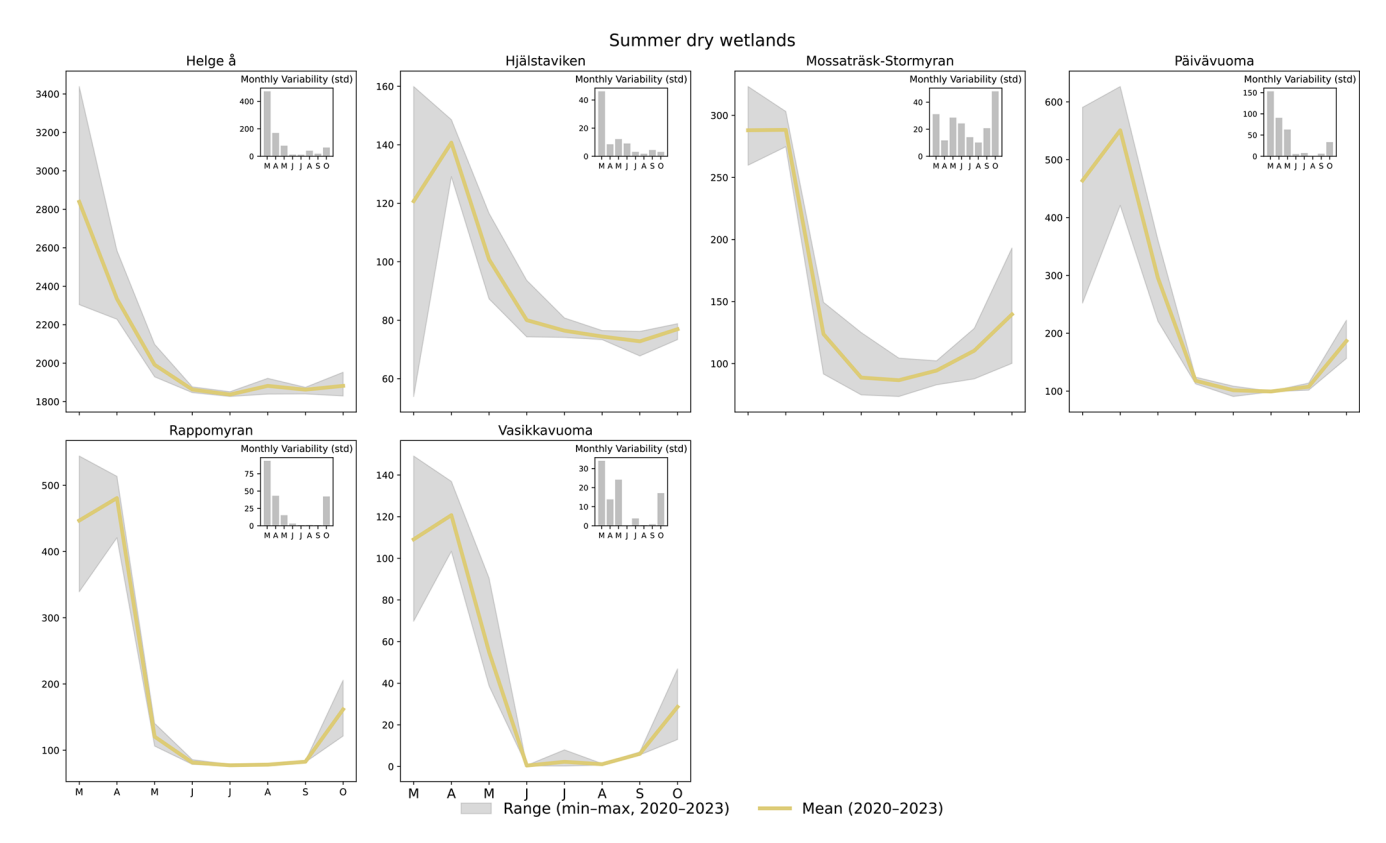


Figure A6. Average monthly water extent (March–October) between 2020–2023 for all wetlands belonging to the summer-dry archetype. Grey area shows the monthly interannual variability given by the range of water extent from all years. The monthly standard deviation is given in the top-right bar plots.

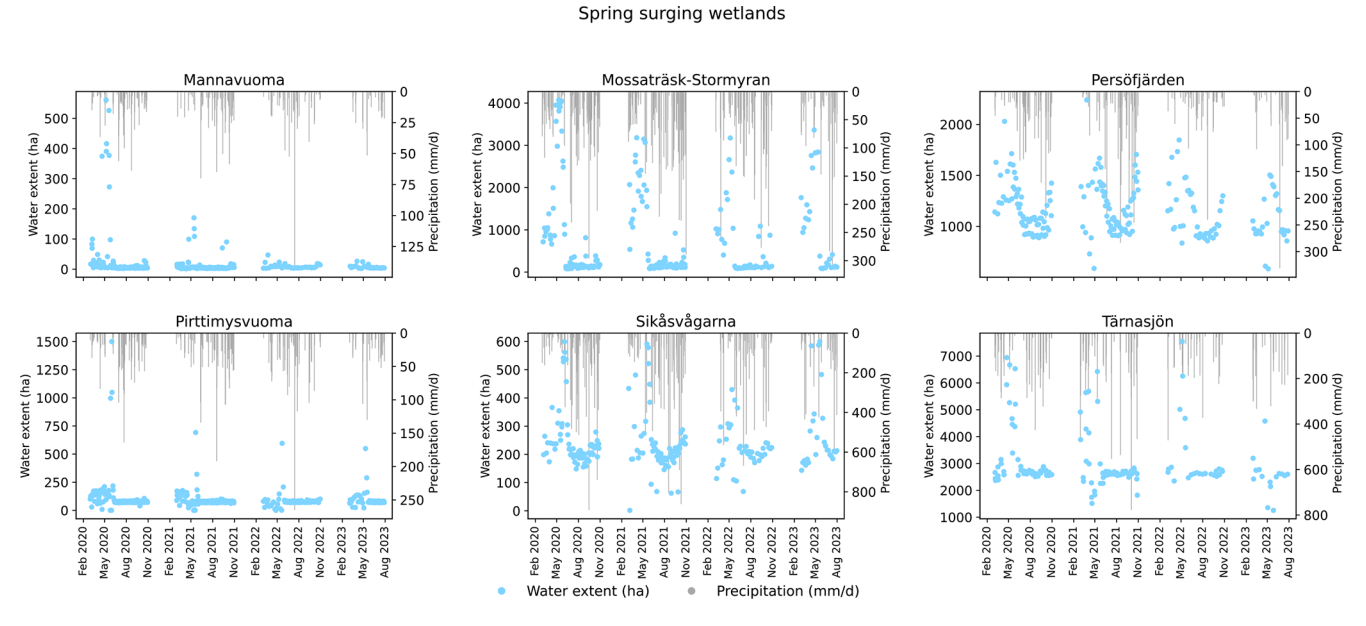


Figure A7. Wetland water extent from January 2020 to August 2023 (excluding January, February, November, and December) for spring-surging wetlands, shown alongside daily precipitation totals for matching dates. Precipitation is aggregated separately for each wetland's catchment and Ramsar area.

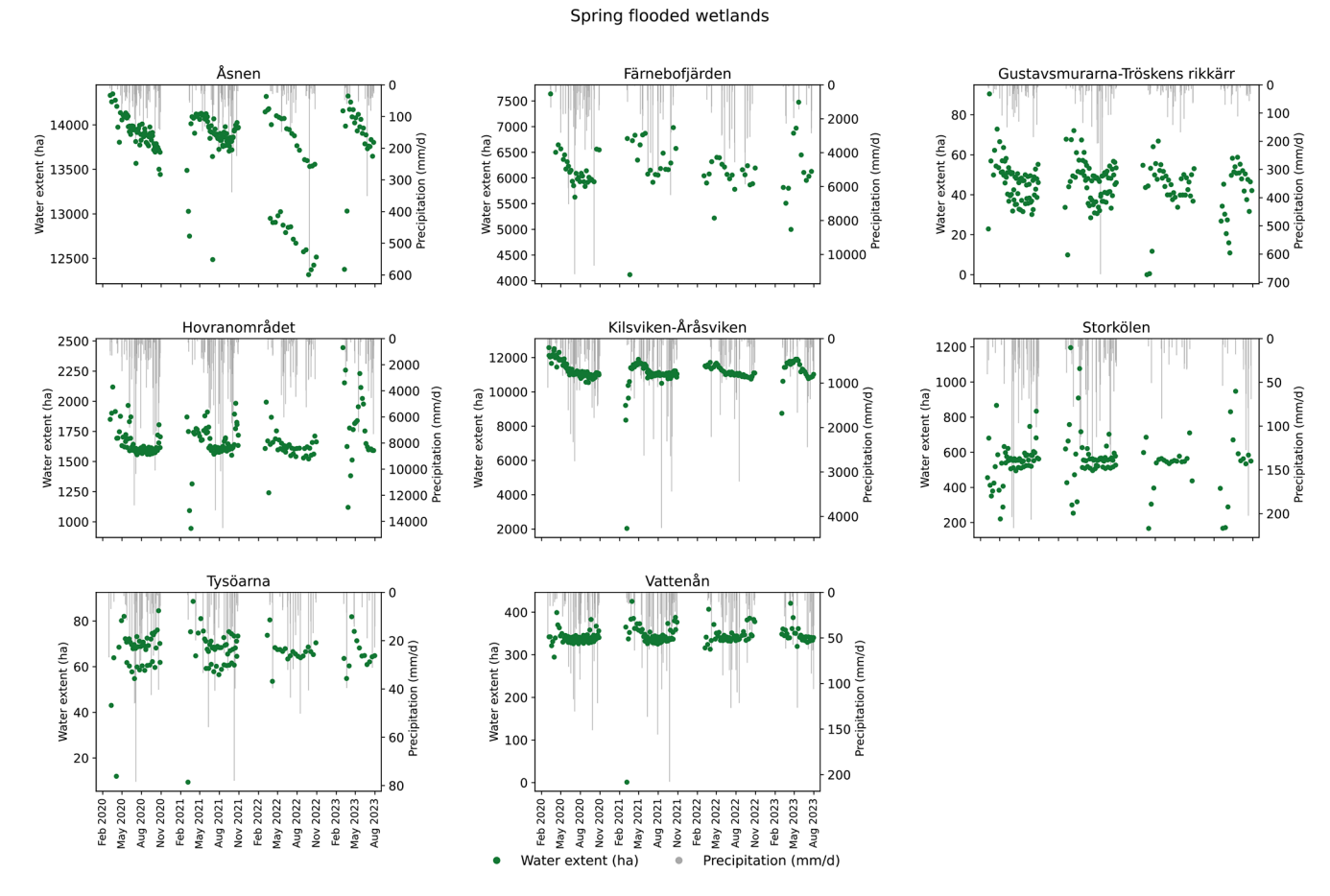


Figure A8. Wetland water extent from January 2020 to August 2023 (excluding January, February, November, and December) for spring-flooded wetlands, shown alongside daily precipitation totals for matching dates. Precipitation is aggregated separately for each wetland's catchment and Ramsar area.

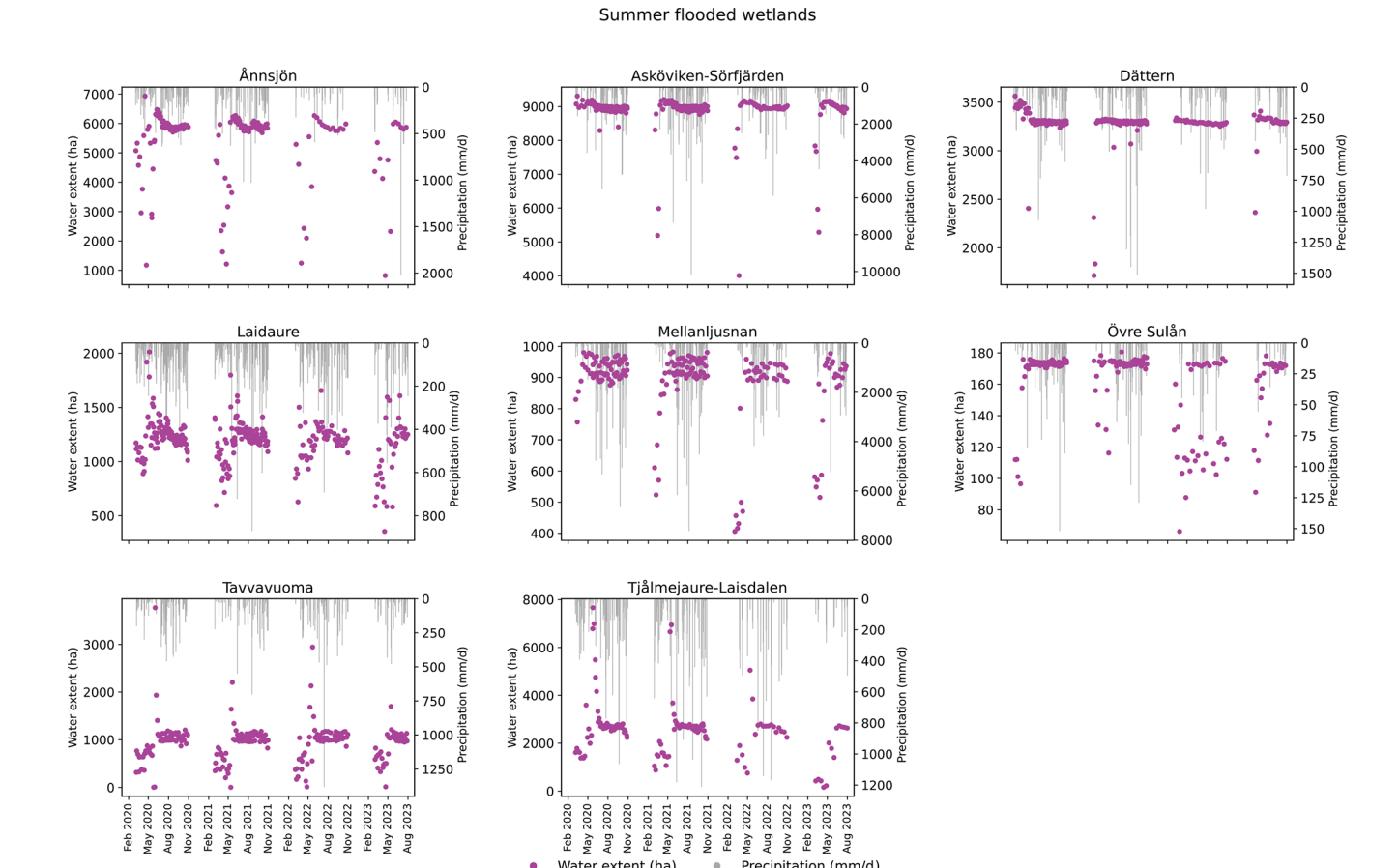


Figure A9. Wetland water extent from January 2020 to August 2023 (excluding January, February, November, and December) for summerflooded wetlands, shown alongside daily precipitation totals for matching dates. Precipitation is aggregated separately for each wetland's catchment and Ramsar area.

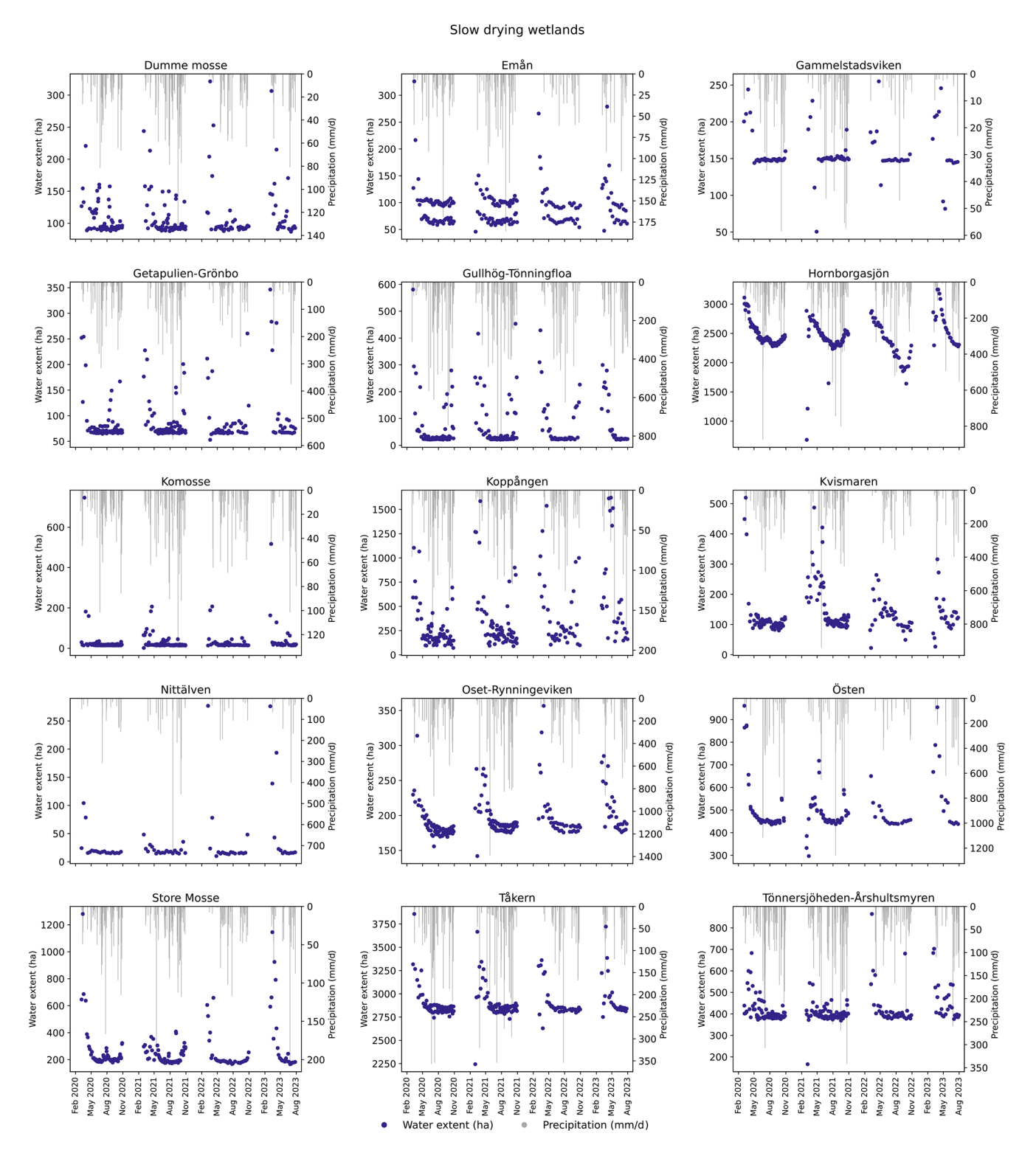


Figure A10. Wetland water extent from January 2020 to August 2023 (excluding January, February, November, and December) for slow-drying wetlands, shown alongside daily precipitation totals for matching dates. Precipitation is aggregated separately for each wetland's catchment and Ramsar area.

Summer dry wetlands

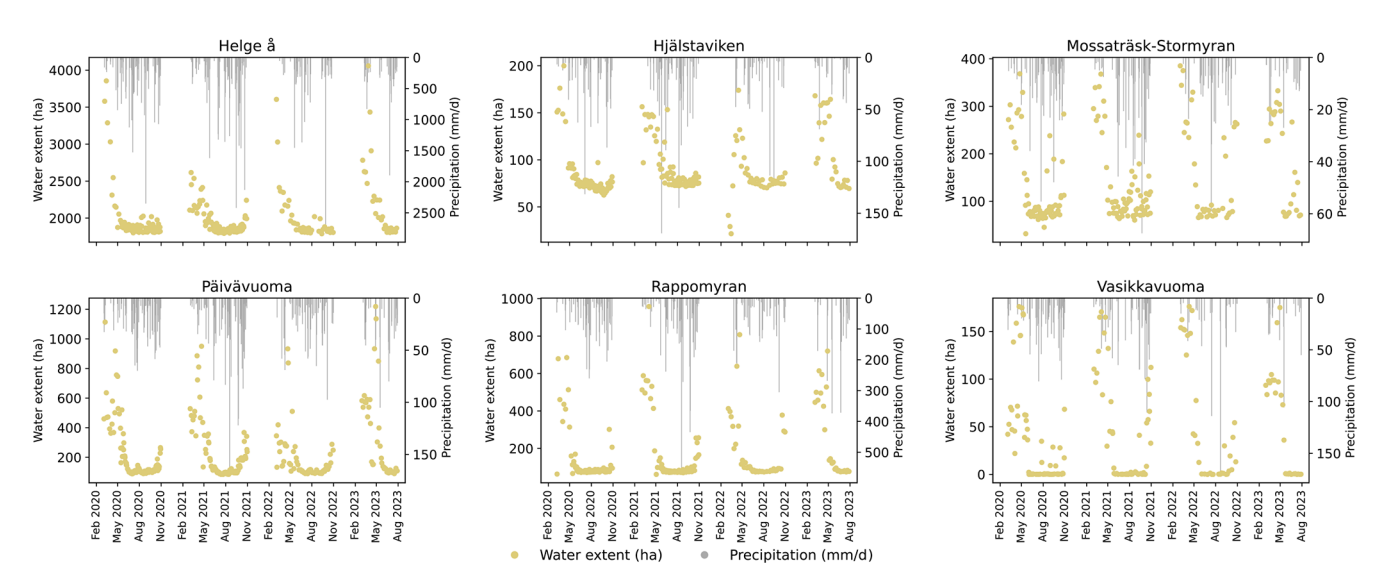


Figure A11. Wetland water extent from January 2020 to August 2023 (excluding January, February, November, and December) for summerdry wetlands, shown alongside daily precipitation totals for matching dates. Precipitation is aggregated separately for each wetland's catchment and Ramsar area.

Code and data availability. All data including environmental data, hydrological parameter results, and water extent data for all wetlands are available through Robinson (2024) (https://doi.org/10.5281/zenodo.16895265). Code for processing data and cluster analysis is available at https://doi.org/10.5281/zenodo.17424880 (Robinson, 2025). Code for predicting water extent in wetlands using DeepAqua can be found at https://doi.org/10.1016/j.jag.2023.103624 (Peña et al., 2024).

Author contributions. AR conceptualized the project, developed the methodology, and conducted data collection and analysis. AS and FP contributed to methodology development and provided research guidance. PH assisted in results interpretation. FJ provided guidance on methodology, data analysis, and interpretation and supervised the project. The co-authors all contributed to the preparation of the paper. The use of ChatGPT helped to improve prose.

Competing interests. The contact author has declared that none of the authors has any competing interests.

Disclaimer. Publisher's note: Copernicus Publications remains neutral with regard to jurisdictional claims made in the text, published maps, institutional affiliations, or any other geographical representation in this paper. While Copernicus Publications makes every effort to include appropriate place names, the final responsibility lies with the authors. Views expressed in the text are those of the authors and do not necessarily reflect the views of the publisher.

Acknowledgements. We acknowledge the E-OBS dataset from the EU-FP6 project UERRA (http://www.uerra.eu, last access: 29 October 2025) and the Copernicus Climate Change Service and the data providers in the ECA&D project (https://www.ecad.eu, last access: 29 October 2025). ChatGPT was used to improve prose in an earlier version of the manuscript.

Financial support. This research has been supported by the Svenska Forskningsrådet Formas (grant no. 2022-01570) and by the project DOWES "Disclosing the Overlooked Wetlandscape Ecosystem Services" of the Water4All 2023 Joint Transnational Call on Aquatic Ecosystem Services, handled by FORMAS with project number 2024-00999.

The publication of this article was funded by the Swedish Research Council, Forte, Formas, and Vinnova.

Review statement. This paper was edited by Bob Su and reviewed by two anonymous referees.

References

Acreman, M. and Holden, J.: How Wetlands Affect Floods, Wetlands, 33, 773–786, https://doi.org/10.1007/s13157-013-0473-2, 2013

Adeli, S., Salehi, B., Mahdianpari, M., Quackenbush, L. J., and Chapman, B.: Moving Toward L-Band NASA-ISRO SAR Mission (NISAR) Dense Time Series: Multipolariza-

- tion Object-Based Classification of Wetlands Using Two Machine Learning Algorithms, Earth and Space Science, 8, https://doi.org/10.1029/2021EA001742, 2021.
- Åhlén, I., Hambäck, P., Thorslund, J., Frampton, A., Destouni, G., and Jarsjö, J.: Wetlandscape size thresholds for ecosystem service delivery: Evidence from the Norrström drainage basin, Sweden, Science of The Total Environment, 704, 135452, https://doi.org/10.1016/j.scitotenv.2019.135452, 2020.
- Åhlén, I., Vigouroux, G., Destouni, G., Pietroń, J., Ghajarnia, N., Anaya, J., Blanco, J., Borja, S., Chalov, S., Chun, K. P., Clerici, N., Desormeaux, A., Girard, P., Gorelits, O., Hansen, A., Jaramillo, F., Kalantari, Z., Labbaci, A., Licero-Villanueva, L., Livsey, J., Maneas, G., Pisarello, K. L. M., Pahani, D. M., Palomino-Ángel, S., Price, R., Ricaurte-Villota, C., Fernanda Ricaurte, L., Rivera-Monroy, V. H., Rodriguez, A., Rodriguez, E., Salgado, J., Sannel, B., Seifollahi-Aghmiuni, S., Simard, M., Sjöberg, Y., Terskii, P., Thorslund, J., Zamora, D. A., and Jarsjö, J.: Hydro-climatic changes of wetlandscapes across the world, Sci. Rep., 11, 2754, https://doi.org/10.1038/s41598-021-81137-3, 2021.
- Åhlén, I., Thorslund, J., Hambäck, P., Destouni, G., and Jarsjö, J.: Wetland position in the landscape: Impact on water storage and flood buffering, Ecohydrology, 15, e2458, https://doi.org/10.1002/eco.2458, 2022.
- Ameli, A. A. and Creed, I. F.: Quantifying hydrologic connectivity of wetlands to surface water systems, Hydrol. Earth Syst. Sci., 21, 1791–1808, https://doi.org/10.5194/hess-21-1791-2017, 2017.
- Ameli, A. A. and Creed, I. F.: Does Wetland Location Matter When Managing Wetlands for Watershed-Scale Flood and Drought Resilience?, JAWRA Journal of the American Water Resources Association, 55, 529–542, https://doi.org/10.1111/1752-1688.12737, 2019.
- Andersson, K.: Multifunctional Wetlands and Stakeholder Engagement: Lessons from Sweden, Stockholm Environment Institute, https://www.sei.org/mediamanager/documents/Publications/ Air-land-water-resources/sei-wp-2012-08-sweden-wetlands. pdf (last access: 20 September 2024), 2012.
- Barbier, E. B., Acreman, M., and Knowler, D.: Economic valuation of wetlands: a guide for policy makers and planners, https://www.ramsar.org/sites/default/files/documents/pdf/lib/lib_valuation_e.pdf (last access: 30 June 2023), 1997.
- Brown, C. F., Brumby, S. P., Guzder-Williams, B., Birch, T., Hyde, S. B., Mazzariello, J., Czerwinski, W., Pasquarella, V. J., Haertel, R., Ilyushchenko, S., Schwehr, K., Weisse, M., Stolle, F., Hanson, C., Guinan, O., Moore, R., and Tait, A. M.: Dynamic World, Near real-time global 10 m land use land cover mapping, Sci. Data, 9, 251, https://doi.org/10.1038/s41597-022-01307-4, 2022.
- Bullock, A. and Acreman, M.: The role of wetlands in the hydrological cycle, Hydrol. Earth Syst. Sci., 7, 358–389, https://doi.org/10.5194/hess-7-358-2003, 2003.
- Canisius, F., Brisco, B., Murnaghan, K., Van Der Kooij, M., and Keizer, E.: SAR Backscatter and InSAR Coherence for Monitoring Wetland Extent, Flood Pulse and Vegetation: A Study of the Amazon Lowland, Remote Sensing, 11, 720, https://doi.org/10.3390/rs11060720, 2019.
- Swedish Meteorological and Hydrological Institute (SMHI): Climate indicator Snow, https://www.smhi.se/en/climate/

- climate-indicators/climate-indicator-snow-1.188971, last access: 8 May 2024.
- Colvin, S. A. R., Sullivan, S. M. P., Shirey, P. D., Colvin, R. W., Winemiller, K. O., Hughes, R. M., Fausch, K. D., Infante, D. M., Olden, J. D., Bestgen, K. R., Danehy, R. J., and Eby, L.: Headwater Streams and Wetlands are Critical for Sustaining Fish, Fisheries, and Ecosystem Services, Fisheries, 44, 73–91, https://doi.org/10.1002/fsh.10229, 2019.
- Cornes, R. C., Van Der Schrier, G., Van Den Besselaar, E. J. M., and Jones, P. D.: An Ensemble Version of the E-OBS Temperature and Precipitation Data Sets, JGR Atmospheres [data set], 123, 9391–9409, https://doi.org/10.1029/2017JD028200, 2018.
- Cuevas, J. G., Valladares, M., Glasner, L., Bresciani, E., Núñez, P., Rojas, J. L., and González, M.: Varied hydrological regime of a semi-arid coastal wetland, Journal of Hydrology and Hydromechanics, 72, 238–251, https://doi.org/10.2478/johh-2024-0007, 2024.
- Cutler, A. and Breiman, L.: Archetypal Analysis, Technometrics, 36, 338–347, https://doi.org/10.1080/00401706.1994.10485840, 1994.
- Davidson, N. C., Dam, A. A. van, Finlayson, C. M., and McInnes, R. J.: Worth of wetlands: revised global monetary values of coastal and inland wetland ecosystem services, Mar. Freshwater Res., 70, 1189–1194, https://doi.org/10.1071/MF18391, 2019.
- Doherty, J. M., Miller, J. F., Prellwitz, S. G., Thompson, A. M., Loheide, S. P., and Zedler, J. B.: Hydrologic Regimes Revealed Bundles and Tradeoffs Among Six Wetland Services, Ecosystems, 17, 1026–1039, https://doi.org/10.1007/s10021-014-9775-3, 2014.
- Everitt, B. S., Landau, S., Leese, M., and Stahl, D.: Cluster Analysis, 1st edn., Wiley, https://doi.org/10.1002/9780470977811, 2011.
- Fluet-Chouinard, E., Stocker, B. D., Zhang, Z., Malhotra, A., Melton, J. R., Poulter, B., Kaplan, J. O., Goldewijk, K. K., Siebert, S., Minayeva, T., Hugelius, G., Joosten, H., Barthelmes, A., Prigent, C., Aires, F., Hoyt, A. M., Davidson, N., Finlayson, C. M., Lehner, B., Jackson, R. B., and McIntyre, P. B.: Extensive global wetland loss over the past three centuries, Nature, 614, 281–286, https://doi.org/10.1038/s41586-022-05572-6, 2023.
- Gerakēs, P. A.: Conservation and Management of Greek Wetlands, in: Proceedings of a Workshop on Greek Wetlands, Thessaloniki, Greece, 17–21 April, 1989, IUCN, 512 pp., https://portals.iucn.org/library/sites/library/files/documents/WTL-002.pdf (last access: 28 March 2024), 1992.
- Golden, H. E., Lane, C. R., Rajib, A., and Wu, Q.: Improving global flood and drought predictions: integrating non-floodplain wetlands into watershed hydrologic models, Environ. Res. Lett., 16, 091002, https://doi.org/10.1088/1748-9326/ac1fbc, 2021.
- Graversgaard, M., Jacobsen, B. H., Hoffmann, C. C., Dalgaard, T., Odgaard, M. V., Kjaergaard, C., Powell, N., Strand, J. A., Feuerbach, P., and Tonderski, K.: Policies for wetlands implementation in Denmark and Sweden historical lessons and emerging issues, Land Use Policy, 101, 105206, https://doi.org/10.1016/j.landusepol.2020.105206, 2021.
- Gunnarsson, U. and Löfroth, M.: Våtmarksinventeringen: resultat från 25 års inventeringar; nationell slutrapport för våtmarksinventeringen (VMI) i Sverige, Naturvårdsverket, Stockholm, 119 pp., https://www.naturvardsverket.se/globalassets/

- media/publikationer-pdf/5900/978-91-620-5925-5.pdf (last access: June 2024), 2009.
- Gunnarsson, U. and Löfroth, M.: The Swedish Wetland Survey: Compiled Excerpts From The National Final Report, Naturvårdsverket [data set], https://www.diva-portal.org/smash/record.jsf?pid=diva2:1609890&dswid=-9307 (last access: 29 October 2025), 2014.
- Hahn, N. and Wester, K.: Satellitbaserad kartering av vegetationstyper inom öppen våtmark, Naturvårdsverket, 2023.
- Hamoudzadeh, A., Ravanelli, R., and Crespi, M.: SWOT Level 2 Lake Single-Pass Product: The L2_HR_LakeSP Data Preliminary Analysis for Water Level Monitoring, Remote Sensing, 16, 1244, https://doi.org/10.3390/rs16071244, 2024.
- Hansson, L.-A., Brönmark, C., Anders Nilsson, P., and Åbjörnsson, K.: Conflicting demands on wetland ecosystem services: nutrient retention, biodiversity or both?, Freshwater Biology, 50, 705– 714, https://doi.org/10.1111/j.1365-2427.2005.01352.x, 2005.
- Helmschrot, J.: Surface Water and the Maintenance of Hydrological Regimes, in: The Wetland Book, edited by: Finlayson, C. M., Everard, M., Irvine, K., McInnes, R. J., Middleton, B. A., Van Dam, A. A., and Davidson, N. C., Springer Netherlands, Dordrecht, 1–10, https://doi.org/10.1007/978-94-007-6172-8_233-2, 2016.
- Huggins, X., Gleeson, T., Villholth, K. G., Rocha, J. C., and Famiglietti, J. S.: Groundwaterscapes: A Global Classification and Mapping of Groundwater's Large-Scale Socioeconomic, Ecological, and Earth System Functions, Water Resources Research, 60, e2023WR036287, https://doi.org/10.1029/2023WR036287, 2024.
- Jaramillo, F., Licero, L., Åhlen, I., Manzoni, S., Rodríguez-Rodríguez, J. A., Guittard, A., Hylin, A., Bolaños, J., Jawitz, J., Wdowinski, S., Martínez, O., and Espinosa, L. F.: Effects of Hydroclimatic Change and Rehabilitation Activities on Salinity and Mangroves in the Ciénaga Grande de Santa Marta, Colombia, Wetlands, 38, 755–767, https://doi.org/10.1007/s13157-018-1024-7, 2018.
- Jaramillo, F., Desormeaux, A., Hedlund, J., Jawitz, J., Clerici, N., Piemontese, L., Rodríguez-Rodriguez, J., Anaya, J., Blanco-Libreros, J., Borja, S., Celi, J., Chalov, S., Chun, K., Cresso, M., Destouni, G., Dessu, S., Di Baldassarre, G., Downing, A., Espinosa, L., Ghajarnia, N., Girard, P., Gutiérrez, Á., Hansen, A., Hu, T., Jarsjö, J., Kalantari, Z., Labbaci, A., Licero-Villanueva, L., Livsey, J., Machotka, E., McCurley, K., Palomino-Ángel, S., Pietron, J., Price, R., Ramchunder, S., Ricaurte-Villota, C., Ricaurte, L., Dahir, L., Rodríguez, E., Salgado, J., Sannel, A., Santos, A., Seifollahi-Aghmiuni, S., Sjöberg, Y., Sun, L., Thorslund, J., Vigouroux, G., Wang-Erlandsson, L., Xu, D., Zamora, D., Ziegler, A., and Åhlén, I.: Priorities and Interactions of Sustainable Development Goals (SDGs) with Focus on Wetlands, Water, 11, 619, https://doi.org/10.3390/w11030619, 2019.
- Jaramillo, F., Aminjafari, S., Castellazzi, P., Fleischmann, A., Fluet-Chouinard, E., Hashemi, H., Hubinger, C., Martens, H. R., Papa, F., Schöne, T., Tarpanelli, A., Virkki, V., Wang-Erlandsson, L., Abarca-del-Rio, R., Borsa, A., Destouni, G., Di Baldassarre, G., Moore, M.-L., Posada-Marín, J. A., Wdowinski, S., Werth, S., Allen, G. H., Argus, D., Elmi, O., Fenoglio, L., Frappart, F., Huggins, X., Kalantari, Z., Munier, S., Palomino-Ángel, S., Robinson, A., Rubiano, K., Siles, G., Simard, M., Song, C., Spence, C., Tourian, M. J., Wada, Y., Wang, C., Wang, J., Yao, F., Berghuijs, W. R., Cretaux, J.-F., Famiglietti, J., Fassoni-

- Andrade, A., Fayne, J. V., Girard, F., Kummu, M., Larson, K. M., Marañon, M., Moreira, D. M., Nielsen, K., Pavelsky, T., Pena, F., Reager, J. T., Rulli, M. C., and Salazar, J. F.: The Potential of Hydrogeodesy to Address Water-Related and Sustainability Challenges, Water Resources Research, 60, e2023WR037020, https://doi.org/10.1029/2023WR037020, 2024.
- Johansson, B.: Estimation of areal precipitation for hydrological modelling in Sweden, https://gupea.ub.gu.se/handle/2077/15575 (last access: 29 August 2024), 2002.
- Johnston, C. A.: Sediment and nutrient retention by freshwater wetlands: Effects on surface water quality, Critical Reviews in Environmental Control, 21, 491–565, https://doi.org/10.1080/10643389109388425, 1991.
- Kadykalo, A. N. and Findlay, C. S.: The flow regulation services of wetlands, Ecosystem Services, 20, 91–103, https://doi.org/10.1016/j.ecoser.2016.06.005, 2016.
- Kirpotin, S., Polishchuk, Y., Bryksina, N., Sugaipova, A., Kouraev, A., Zakharova, E., Pokrovsky, O. S., Shirokova, L., Kolmakova, M., Manassypov, R., and Dupre, B.: West Siberian palsa peatlands: distribution, typology, cyclic development, present day climate-driven changes, seasonal hydrology and impact on CO₂ cycle, International Journal of Environmental Studies, 68, 603–623, https://doi.org/10.1080/00207233.2011.593901, 2011.
- Kovacs, J. M., Lu, X. X., Flores-Verdugo, F., Zhang, C., Flores de Santiago, F., and Jiao, X.: Applications of ALOS PALSAR for monitoring biophysical parameters of a degraded black mangrove (Avicennia germinans) forest, ISPRS Journal of Photogrammetry and Remote Sensing, 82, 102–111, https://doi.org/10.1016/j.isprsjprs.2013.05.004, 2013.
- Lane, C. R., Leibowitz, S. G., Autrey, B. C., LeDuc, S. D., and Alexander, L. C.: Hydrological, Physical, and Chemical Functions and Connectivity of Non-Floodplain Wetlands to Downstream Waters: A Review, JAWRA Journal of the American Water Resources Association, 54, 346–371, https://doi.org/10.1111/1752-1688.12633, 2018.
- Lantmateriet: Produktbeskrivning: Markhöjdmodell Nedladdning, grid 50+ NH [data set], https://www. lantmateriet.se/sv/geodata/vara-produkter/produktlista/ markhojdmodell-nedladdning-grid-50/ (last access: 5 August 2024), 2022.
- Le, P. V. V. and Kumar, P.: Power law scaling of topographic depressions and their hydrologic connectivity, Geophysical Research Letters, 41, 1553–1559, https://doi.org/10.1002/2013GL059114, 2014.
- Magilligan, F. J. and Nislow, K. H.: Changes in hydrologic regime by dams, Geomorphology, 71, 61–78, https://doi.org/10.1016/j.geomorph.2004.08.017, 2005.
- Margaryan, L., Prince, S., Ioannides, D., and Röslmaier, M.: Dancing with cranes: a humanist perspective on cultural ecosystem services of wetlands, Tourism Geographies, 24, 501–522, https://doi.org/10.1080/14616688.2018.1522512, 2022.
- Matthew, M., Lisa-Maria, R., Sonali, S. S., and de Sanjiv, S.: Wetlands, agriculture and poverty reduction, IWMI, 44 pp., https://cgspace.cgiar.org/server/api/core/bitstreams/a9396ccc-acc9-4028-953f-b52875de4333/content (last access: 30 June 2023), 2010.
- Matti, B., Dahlke, H. E., Dieppois, B., Lawler, D. M., and Lyon, S. W.: Flood seasonality across Scandinavia Evidence of a

- shifting hydrograph?, Hydrological Processes, 31, 4354–4370, https://doi.org/10.1002/hyp.11365, 2017.
- McLaughlin, D. L. and Cohen, M. J.: Realizing ecosystem services: wetland hydrologic function along a gradient of ecosystem condition, Ecological Applications, 23, 1619–1631, https://doi.org/10.1890/12-1489.1, 2013.
- Melack, J. M. and Hess, L. L.: Remote Sensing of the Distribution and Extent of Wetlands in the Amazon Basin, in: Amazonian Floodplain Forests: Ecophysiology, Biodiversity and Sustainable Management, edited by: Junk, W. J., Piedade, M. T. F., Wittmann, F., Schöngart, J., and Parolin, P., Springer Netherlands, Dordrecht, 43–59, https://doi.org/10.1007/978-90-481-8725-6_3, 2011.
- Mitsch, W. J., Taylor, J. R., and Benson, K. B.: Estimating primary productivity of forested wetland communities in different hydrologic landscapes, Landscape Ecol., 5, 75–92, https://doi.org/10.1007/BF00124662, 1991.
- Mitsch, W. J., Bernal, B., and Hernandez, M. E.: Ecosystem services of wetlands, International Journal of Biodiversity Science, Ecosystem Services & Management, 11, 1–4, https://doi.org/10.1080/21513732.2015.1006250, 2015.
- Morley, T. R., Reeve, A. S., and Calhoun, A. J. K.: The Role of Headwater Wetlands in Altering Streamflow and Chemistry in a Maine, USA Catchment, JAWRA Journal of the American Water Resources Association, 47, 337–349, https://doi.org/10.1111/j.1752-1688.2010.00519.x, 2011.
- Mupepi, O., Marambanyika, T., Matsa, M. M., and Dube, T.: A systematic review on remote sensing of wetland environments, Transactions of the Royal Society of South Africa, 79, 67–85, https://doi.org/10.1080/0035919X.2024.2322946, 2024.
- Na, X. and Li, W.: Modeling Hydrological Regimes of Floodplain Wetlands Using Remote Sensing and Field Survey Data, Water, 14, 4126, https://doi.org/10.3390/w14244126, 2022.
- Okruszko, T., Duel, H., Acreman, M., Grygoruk, M., Flörke, M., and Schneider, C.: Broad-scale ecosystem services of European wetlands overview of the current situation and future perspectives under different climate and water management scenarios, Hydrological Sciences Journal, 56, 1501–1517, https://doi.org/10.1080/02626667.2011.631188, 2011.
- Olden, J. D. and Poff, N. L.: Redundancy and the choice of hydrologic indices for characterizing streamflow regimes, River Research and Applications, 19, 101–121, https://doi.org/10.1002/rra.700, 2003.
- Opperman, J. J., Luster, R., McKenney, B. A., Roberts, M., and Meadows, A. W.: Ecologically Functional Floodplains: Connectivity, Flow Regime, and Scale, JAWRA Journal of the American Water Resources Association, 46, 211–226, https://doi.org/10.1111/j.1752-1688.2010.00426.x, 2010.
- Otsu, N.: A Threshold Selection Method from Gray-Level Histograms, IEEE Transactions on Systems, Man, and Cybernetics, 9, 62–66, https://doi.org/10.1109/TSMC.1979.4310076, 1979.
- Park, J., Kumar, M., Lane, C. R., and Basu, N. B.: Seasonality of inundation in geographically isolated wetlands across the United States, Environ. Res. Lett., 17, 054005, https://doi.org/10.1088/1748-9326/ac6149, 2022.
- Peña, F. J., Hübinger, C., Payberah, A. H., and Jaramillo, F.: DeepAqua: Semantic segmentation of wetland water surfaces with SAR imagery using deep neural networks without manually annotated data, International Journal of Applied

- Earth Observation and Geoinformation [code], 126, 103624, https://doi.org/10.1016/j.jag.2023.103624, 2024.
- Piemontese, L., Castelli, G., Fetzer, I., Barron, J., Liniger, H., Harari, N., Bresci, E., and Jaramillo, F.: Estimating the global potential of water harvesting from successful case studies, Global Environmental Change, 63, https://doi.org/10.1016/j.gloenvcha.2020.102121, 2020.
- Poff, N. L., Allan, J. D., Bain, M. B., Karr, J. R., Prestegaard, K. L., Richter, B. D., Sparks, R. E., and Stromberg, J. C.: The Natural Flow Regime, BioScience, 47, 769–784, https://doi.org/10.2307/1313099, 1997.
- Prigent, C., Matthews, E., Aires, F., and Rossow, W. B.: Remote sensing of global wetland dynamics with multiple satellite data sets, Geophysical Research Letters, 28, 4631–4634, 2001.
- Ramsar Convention Secretariat: The Convention on Wetlands of International Importance, especially as Waterfowl Habitat, Ramsar, Iran, 2 February 1971, https://www.ramsar.org/, last access: 23 October 2025
- Ramsar Convention (Ed.): The use of Earth Observation for wetland inventory, assessment and monitoring, in: Wetlands, Springer Netherlands, Dordrecht, 189–203, https://doi.org/10.1007/978-94-007-0551-7_11, 2011.
- Ramsar Convention Secretariat: Ramsar Sites in Sweden, https://www.ramsar.org/wetland/sweden, last access: 28 June 2023.
- Ringeval, B., de Noblet-Ducoudré, N., Ciais, P., Bousquet, P., Prigent, C., Papa, F., and Rossow, W. B.: An attempt to quantify the impact of changes in wetland extent on methane emissions on the seasonal and interannual time scales, Global Biogeochemical Cycles, 24, https://doi.org/10.1029/2008GB003354, 2010.
- Robinson, A.: Supplementary data, Zenodo [data set], https://doi.org/10.5281/zenodo.16895265, 2024.
- Robinson, A: Hydrological_archetypes, Zenodo [code], https://doi.org/10.5281/zenodo.17424880, 2025.
- Robinson, J. S. and Sivapalan, M.: Temporal scales and hydrological regimes: Implications for flood frequency scaling, Water Resources Research, 33, 2981–2999, https://doi.org/10.1029/97WR01964, 1997.
- Spence, C., Guan, X. J., and Phillips, R.: The Hydrological Functions of a Boreal Wetland, Wetlands, 31, 75–85, https://doi.org/10.1007/s13157-010-0123-x, 2011.
- Stevaux, J. C., Macedo, H. de A., Assine, M. L., and Silva, A.: Changing fluvial styles and backwater flooding along the Upper Paraguay River plains in the Brazilian Pantanal wetland, Geomorphology, 350, 106906, https://doi.org/10.1016/j.geomorph.2019.106906, 2020.
- Swedish Meteorological and Hydrological Institute (SMHI): Water discharge data, SMHI [data set], https://www.smhi.se/data/sjoar-och-vattendrag/vattenforing/waterdischargeDaily/2612, last access: 23 October 2025.
- Tang, Y., Leon, A. S., and Kavvas, M. L.: Impact of Size and Location of Wetlands on Watershed-Scale Flood Control, Water Resour. Manage., 34, 1693–1707, https://doi.org/10.1007/s11269-020-02518-3, 2020.
- The Global Runoff Data Centre (GRDC): The Global Runoff Data Centre, 56068 Koblenz, Germany, GRDC [data set], https://grdc.bafg.de/, last access: 23 October 2025.

- Vera-Herrera, L., Soria, J., Pérez, J., and Romo, S.: Long-Term Hydrological Regime Monitoring of a Mediterranean Agro-Ecological Wetland Using Landsat Imagery: Correlation with the Water Renewal Rate of a Shallow Lake, Hydrology, 8, 172, https://doi.org/10.3390/hydrology8040172, 2021.
- Vilardy, S. P., González, J. A., Martín-López, B., and Montes, C.: Relationships between hydrological regime and ecosystem services supply in a Caribbean coastal wetland: a socialecological approach, Hydrological Sciences Journal, 56, 1423– 1435, https://doi.org/10.1080/02626667.2011.631497, 2011.
- Villa, J. A. and Mitsch, W. J.: Carbon sequestration in different wetland plant communities in the Big Cypress Swamp region of southwest Florida, International Journal of Biodiversity Science, Ecosystem Services & Management, 11, 17–28, https://doi.org/10.1080/21513732.2014.973909, 2015.
- Votrubova, J., Dohnal, M., Vogel, T., Sanda, M., and Tesar, M.: Episodic runoff generation at Central European headwater catchments studied using water isotope concentration signals, Journal of Hydrology and Hydromechanics, 65, 114–122, https://doi.org/10.1515/johh-2017-0002, 2017.
- Widhalm, B., Bartsch, A., and Heim, B.: A novel approach for the characterization of tundra wetland regions with C-band SAR satellite data, International Journal of Remote Sensing, 36, 5537– 5556, https://doi.org/10.1080/01431161.2015.1101505, 2015.
- Winter, T. C.: The Vulnerability of Wetlands to Climate Change: A Hydrologic Landscape Perspective, J. American Water Resour. Assoc., 36, 305–311, https://doi.org/10.1111/j.1752-1688.2000.tb04269.x, 2000.

- Wood, K. A., Jupe, L. L., Aguiar, F. C., Collins, A. M., Davidson, S. J., Freeman, W., Kirkpatrick, L., Lobato-de Magalhães, T., McKinley, E., Nuno, A., Pagès, J. F., Petruzzella, A., Pritchard, D., Reeves, J. P., Thomaz, S. M., Thornton, S. A., Yamashita, H., and Newth, J. L.: A global systematic review of the cultural ecosystem services provided by wetlands, Ecosystem Services, 70, 101673, https://doi.org/10.1016/j.ecoser.2024.101673, 2024.
- Xi, Y., Peng, S., Ciais, P., and Chen, Y.: Future impacts of climate change on inland Ramsar wetlands, Nat. Clim. Chang., 11, 45–51, https://doi.org/10.1038/s41558-020-00942-2, 2021.
- Xu, D., Bisht, G., Tan, Z., Sinha, E., Di Vittorio, A. V., Zhou, T., Ivanov, V. Y., and Leung, L. R.: Climate change will reduce North American inland wetland areas and disrupt their seasonal regimes, Nat. Commun., 15, 2438, https://doi.org/10.1038/s41467-024-45286-z, 2024.
- Yanfeng W. U. and Guangxin Z.: A review of hydrological regulation functions of watershed wetlands, skxjz, 32, 458–469, https://doi.org/10.14042/j.cnki.32.1309.2021.03.014, 2021.
- Zakharova, E. A., Kouraev, A. V., Rémy, F., Zemtsov, V. A., and Kirpotin, S. N.: Seasonal variability of the Western Siberia wetlands from satellite radar altimetry, Journal of Hydrology, 512, 366–378, https://doi.org/10.1016/j.jhydrol.2014.03.002, 2014.
- Zhang, H., Huang, G. H., Wang, D., and Zhang, X.: Uncertainty assessment of climate change impacts on the hydrology of small prairie wetlands, Journal of Hydrology, 396, 94–103, https://doi.org/10.1016/j.jhydrol.2010.10.037, 2011.